Article

Cell Reports

Networks of Cultured iPSC-Derived Neurons Reveal the Human Synaptic Activity-Regulated Adaptive Gene Program

Graphical Abstract

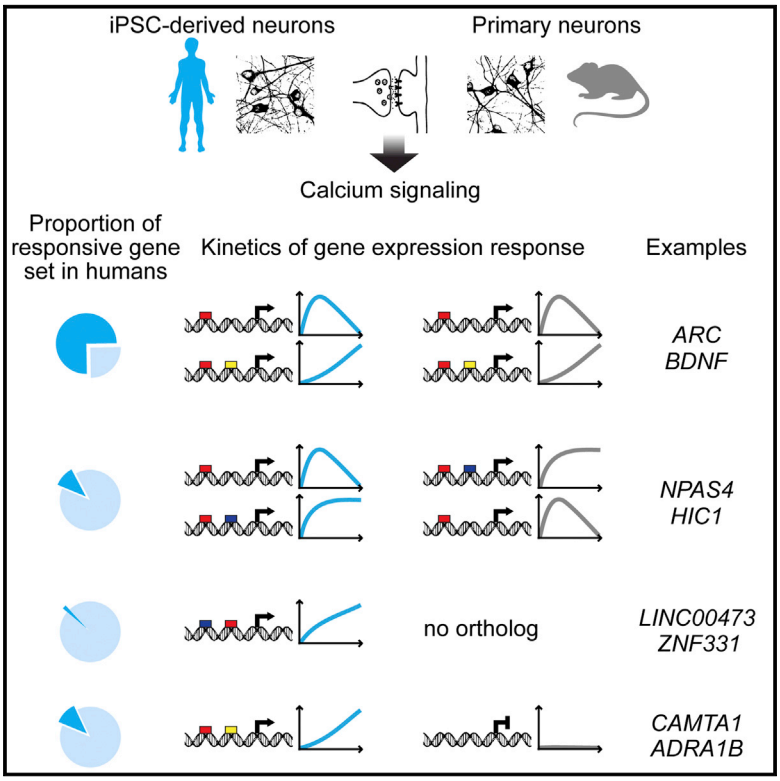

Authors

Priit Pruunsild, C. Peter Bengtson, Hilmar Bading

Correspondence

bading@nbio.uni-heidelberg.de

In Brief

Using comparative analysis of synaptic activity-responsive gene expression programs in human and mouse neuronal networks, Pruunsild et al. uncover differences that are due to lineage-specific acquisition of genes and DNA regulatory elements. Such genetic alterations and the resulting changes in activity-driven transcription may be relevant for the evolution of human cognitive abilities.

Highlights

- The repertoire of human activity-induced genes is expanded lineage specifically
- Temporal expression profiles of many activity-responsive genes are species specific
- Some human orthologs of mouse genes have gained inducibility by synaptic activity
- The human *HIC1* gene promoter has gained an activity-responsive regulatory element

Accession Numbers

GSE88773

Pruunsild et al., 2017, Cell Reports *18*, 122–135
January 3, 2017 © 2017 The Author(s).
http://dx.doi.org/10.1016/j.celrep.2016.12.018

OPEN ACCESS
CellPress

Cell Reports
Article

Networks of Cultured iPSC-Derived Neurons Reveal the Human Synaptic Activity-Regulated Adaptive Gene Program

Priit Pruunsild,[1] C. Peter Bengtson,[1] and Hilmar Bading[1,2,*]
[1]Department of Neurobiology, Interdisciplinary Center for Neurosciences (IZN), Heidelberg University, INF 364, 69120 Heidelberg, Germany
[2]Lead Contact
*Correspondence: bading@nbio.uni-heidelberg.de
http://dx.doi.org/10.1016/j.celrep.2016.12.018

SUMMARY

Long-term adaptive responses in the brain, such as learning and memory, require synaptic activity-regulated gene expression, which has been thoroughly investigated in rodents. Using human iPSC-derived neuronal networks, we show that the human and the mouse synaptic activity-induced transcriptional programs share many genes and both require Ca^{2+}-regulated synapse-to-nucleus signaling. Species-specific differences include the noncoding RNA genes *BRE-AS1* and *LINC00473* and the protein-coding gene *ZNF331*, which are absent in the mouse genome, as well as several human genes whose orthologs are either not induced by activity or are induced with different kinetics in mice. These results indicate that lineage-specific gain of genes and DNA regulatory elements affects the synaptic activity-regulated gene program, providing a mechanism driving the evolution of human cognitive abilities.

INTRODUCTION

Transcription-dependent neuronal plasticity is evolutionarily conserved from invertebrates to mammals (Frank and Greenberg, 1994). Accordingly, the neuronal activity-dependent gene expression program, which underlies adaptation-related brain functions, is likely generic, meaning that many of the activity-responsive genes are shared between species and neuron types (discussed by Bading, 2013). This assumption includes humans. Yet, these genes are poorly characterized in humans, especially in comparison to mice whose activity-regulated transcriptome, implicating ~1,000 genes, is known (Kim et al., 2010; Saha et al., 2011; Spiegel et al., 2014; Zhang et al., 2007, 2009). It is important as well as exciting to fill this gap in knowledge, since, as for phenotypic differences between species in general (Necsulea and Kaessmann, 2014; Wilson and Odom, 2009), evolutionary gene regulation and expression changes may, to a large extent, determine the dissimilarities in brain development and function of humans compared to other species (Bae et al., 2015; Geschwind and Rakic, 2013; Silbereis et al., 2016). Cognitive abilities, which in humans have evolved to a perplexing species-specific phenotype distinction, are in part reliant on synaptic activity-dependent gene regulation (Bading, 2013; West and Greenberg, 2011). In humans, the orthologs of rodent activity-regulated genes are expressed with a species-specific temporal profile during brain development (Liu et al., 2012). Whether the human synaptic activity-regulated gene program itself has distinctive features is unknown, however, mostly because obtaining human neurons for experimental use is ethically problematic. Here we determine the gene expression response to synaptic activity in human neurons derived from induced pluripotent stem cells (iPSCs) to find out if the human genetic background expands the repertoire of known activity-regulated genes.

RESULTS

Studies of the human neuronal adaptive gene program require an experimental system where human neurons are synaptically connected. We differentiated iPSCs (see the Experimental Procedures) to human iPSC-derived (hiPSCd) neurons, and we confirmed the generation of postmitotic neuronal cells by expression analysis of multiple markers, RNA sequencing (RNA-seq), and comparison of the hiPSCd neuron transcriptomes to previously published hiPSCd neuron and human fetal brain gene expression profiles (Figure S1; Table S1).

Electrical Properties and Synaptic Connectivity of Human iPSC-Derived Neurons

To directly assess cellular phenotype on a functional level, we performed whole-cell patch-clamp recordings from hiPSCd neurons differentiated for 7 or 10 weeks from hiPSCd neuronal precursor cells (NPCs) (hereafter 7- or 10-week hiPSCd neurons). At earlier time points, hiPSCd neurons were electrophysiologically immature. In parallel, we recorded from 7-week hiPSCd neurons cultured together with mouse (post-natal day [P]0) primary hippocampal neurons for the last 10 days (hereafter hiPSCd neuron/mouse primary neuron co-culture or mixed-species culture). The hiPSCd neurons in the co-cultures were distinguished by their expression of EGFP under the control of the human *synapsin I* (*SYN1*) promoter (p*SYN1*) delivered by lentiviral infection of NPCs (see also Figures S1C, S1D, and 3G). Passive properties (membrane capacitance [34–38 pF], resistance [900–1,350 MΩ], and resting membrane potential [Vrest, −43 to −48 mV]) of hiPSCd neurons were not affected by co-culture

This is an open access article under the CC BY-NC-ND license (http://creativecommons.org/licenses/by-nc-nd/4.0/).

with mouse neurons (in figures denoted by *Hs* + *Mm*, hiPSCd neuron-only culture is denoted by *Hs*), and they were not significantly different between cells in the 7- and 10-week hiPSCd neuron-only cultures (Figures 1A–1C). The hiPSCd neurons were electrically excitable, fulfilling a key criterion for functional neurons. Action potential (AP) amplitudes and numbers were improved when evoked from −70 mV instead of Vrest (Figures 1D–1F), which reflects their relatively depolarized state.

Almost all hiPSCd neurons in all cultures analyzed showed spontaneous postsynaptic currents that could be divided into two groups, with rapid or slow decay time constants (Figures 1G–1I). They were blocked in EGFP-expressing ($EGFP^+$) cells by either NBQX (5 μM), a blocker of AMPA/kainate-type glutamate receptors (7-week hiPSCd neuron-only cultures or mixed-species cultures, n = 4/4 for each), or by the GABA type A ($GABA_A$) receptor antagonists bicuculline (Bic, 50 μM) or gabazine (5 μM) (7-week hiPSCd neuron-only cultures, n = 7/7; mixed-species cultures, n = 5/5), respectively. This confirms the presence of functional synapses containing postsynaptic AMPA/kainate or $GABA_A$ receptors in our hiPSCd neurons.

To verify the existence of functional NMDA, AMPA, and $GABA_A$ receptors as well as voltage-gated Ca^{2+} channels (VGCCs) in hiPSCd neurons, we used Ca^{2+} imaging. In almost all $EGFP^+$ and EGFP-non-expressing ($EGFP^-$) cells in the 7-week hiPSCd neuron-only cultures, large Ca^{2+} responses were evoked by NMDA, applied with its co-agonist glycine, or by AMPA, applied with an inhibitor of AMPA receptor desensitization, cyclothiazide (Figure 1J). GABA also increased Ca^{2+} levels (Figure 1K), indicating an excitatory, depolarizing effect. Ca^{2+} influx in response to AMPA, NMDA, and GABA presumably involves VGCCs, and their presence in hiPSCd neurons was confirmed by robust increases in Ca^{2+} in response to depolarization with a high-concentration K^+ solution (Figure 1K). Thus, 7 weeks of differentiation of human iPSC-derived NPCs is sufficient to obtain hiPSCd neurons that exhibit functional AMPA, NMDA, and $GABA_A$ receptors as well as VGCCs.

Bicuculline Together with 4-Aminopyridine Increases Synaptic Input to Human iPSC-Derived Neurons

Having established culture systems generating synaptically connected hiPSCd neurons, we sought a method to experimentally induce robust excitatory synaptic activity in these cultures to study activity-induced transcription in hiPSCd neurons. In 10-day cultures of mouse primary hippocampal neurons, synaptic activity-dependent gene expression can be induced by disinhibition of the neuronal network with Bic, which triggers synchronous bursts of AP firing along with AMPA and NMDA receptor- and VGCC-mediated Ca^{2+} signals, whose frequency is increased by coapplication of Bic with the K^+ channel blocker 4-aminopyridine (4AP) (Arnold et al., 2005; Hardingham et al., 2001). Bic (50 μM) applied together with 4AP (250 μM) (Bic/4AP) activated large recurring bursts of synaptic activity in both $EGFP^+$ and $EGFP^-$ cells in our 7-week mixed-species cultures (Figures 2A and 2B) and, to a lesser extent, in 7-week hiPSCd neuron-only cultures (Figure 2C). $EGFP^+$ cells in 7-week hiPSCd neuron-only cultures and mixed-species cultures showed, respectively, a 4.4-fold and a 10.8-fold increase in synaptic charge influx after Bic/4AP treatment (Figure 2E). In the 10-week hiPSCd neuron cultures, Bic/4AP induced larger synaptic bursts than in the 7-week hiPSCd neuron-only cultures (Figures 2C and 2D), and it caused recurring membrane potential oscillations (18.9 ± 1.9 mV; 1.73 ± 0.44/min; n = 8), which were abolished by NBQX (n = 3; data not shown). Synaptic activation caused by Bic/4AP was accompanied by recurrent depolarizations and/or APs in all cultures assessed.

Analyses of Ca^{2+} transients activated downstream of Bic/4AP-induced synaptic activity revealed large, recurrent increases in Ca^{2+} levels with a sustained increase in baseline Ca^{2+} levels in both $EGFP^+$ and $EGFP^-$ cells in the 7-week co-cultures (Figure 2F), similar to responses seen in mouse primary hippocampal neurons (Hardingham et al., 2001). Recurrent Ca^{2+} responses to Bic/4AP also were apparent in 7- and 10-week hiPSCd neuron-only cultures but without a sustained increase in baseline Ca^{2+} levels and with a smaller amplitude in the 7-week than in the 10-week cultures (Figures 2G–2I). The depolarizing effect of GABA (see above) and the lack of response to Bic (Figure S2A) in 7-week hiPSCd neuron-only cultures may explain their weaker responses to Bic/4AP compared to 10-week hiPSCd neurons, where $GABA_A$ receptors likely have undergone the developmental switch from excitatory to inhibitory (Ben-Ari et al., 2007).

These results demonstrate that Bic/4AP induces robust recurrent increases in AMPA/kainate receptor-mediated synaptic and AP activity along with Ca^{2+} influx into hiPSCd neurons in the mixed-species or hiPSCd neuron-only cultures. The addition of mouse primary neurons to the 7-week hiPSCd neuron cultures or the extra 3 weeks of differentiation of hiPSCd neuron-only cultures greatly increase hiPSCd neuron responses to Bic/4AP.

Excitatory Input to Human iPSC-Derived Neurons Induces Human Immediate-Early Genes

We used species-specific RT-qPCR on human orthologs of three prototypical activity-responsive mouse immediate-early (IE) genes, *Npas4*, *Fos*, and *Arc*, to assess if enhancement of synaptic input to hiPSCd neurons induces human IE genes. Increases in human *NPAS4*, *FOS*, and *ARC* mRNA levels in hiPSCd neurons after a 1-hr Bic/4AP treatment were easily detectable in both hiPSCd neurons cultured with or without mouse primary neurons (Figures 3A and 3B). Induction strength of *NPAS4* and *ARC* improved gradually over the NPC differentiation period. All the inductions peaked 1 hr after Bic/4AP addition and dropped almost to the basal levels by 4 hr (Figures 3C and 3D).

In the 7-week co-cultures, the increases in the levels of all of the three assessed human IE gene mRNAs in response to Bic/4AP were abolished in the presence of tetrodotoxin (TTX, 1 μM), an Na^+ channel blocker that prevents Bic/4AP-induced Ca^{2+} signals by inhibiting AP firing (Hardingham et al., 2002), proving that expression of *NPAS4*, *FOS*, and *ARC* is activity-regulated in hiPSCd neurons (Figure 3E). The Bic/4AP-induced increase in *NPAS4* mRNA levels was reduced by the inhibition of L-type VGCCs with Nifedipine (Nif, 10 μM) or by two NMDA receptor antagonists, 2-amino-5-phosphonovalerate (APV, 50 μM) and MK801 (MK, 10 μM) (APV/MK). Induction of *NPAS4* and *FOS* was more strongly inhibited by the combination of Nif, APV, and MK (Nif/APV/MK), revealing a potential synergistic role of VGCCs and NMDA receptors (Figure 3E). In the 10-week hiPSCd

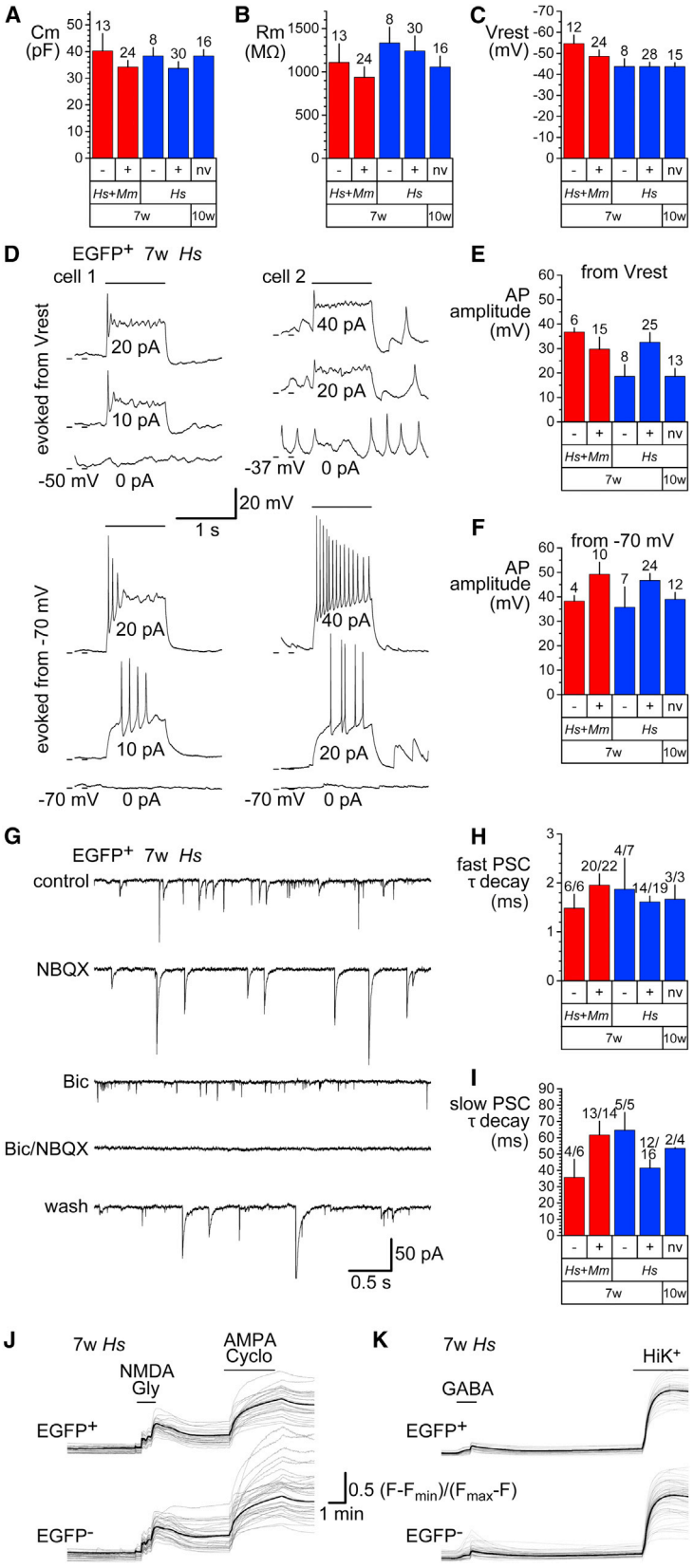

Figure 1. Electrophysiological and Pharmacological Properties of Human iPSCd Neurons

All culture conditions and cell groups analyzed are specified at the end of the figure legend.

(A–C) The (A) cell capacitance (Cm), (B) membrane resistance (Rm), and (C) resting membrane potential (Vrest) were measured with whole-cell patch clamp. Mean ± SEM.

(D) Action potentials (APs) in representative human cells (cell 1 and cell 2). APs were evoked from Vrest or −70 mV with current injection (bar) at the levels indicated.

(E and F) Quantification of AP amplitude evoked from (E) Vrest or (F) −70 mV is shown. Mean ± SEM.

(G) Traces of spontaneous postsynaptic currents (PSCs) at Vhold = −70 mV, in a representative human cell in control conditions, in the presence of NBQX (5 μM) and/or bicuculline (Bic, 50 μM), are shown.

(H and I) Quantification of the decay τ from a single exponential fit for (H) NBQX-sensitive PSCs with rapid decay kinetics and (I) Bic-sensitive PSCs with slow decay kinetics is shown. Mean ± SEM.

(J and K) Traces of Rhod2 Ca^{2+} imaging. Responses to (J) NMDA (100 μM) and glycine (Gly, 20 μM), (J) AMPA (10 μM) and cyclothiazide (Cyclo, 20 μM), (K) GABA (300 μM), and (K) a high-concentration K^+ solution (HiK^+, 45 mM) are shown. Gray lines represent individual cells and black lines are the averages (n = 25–295). No significant differences were detected in (A)–(C), (E), (F), (H), and (I) (three-way ANOVA).

7w or 10w, human NPCs were differentiated for 7 or 10 weeks, respectively; *Hs* + *Mm*, hiPSCd neuron/mouse primary hippocampal neuron co-culture; *Hs*, hiPSCd neuron-only culture; − and $EGFP^-$, mouse cells or human cells that have either not activated p*SYN1* after infection with a lentivirus encoding EGFP under the control of p*SYN1* or were not infected; + and $EGFP^+$, EGFP-positive human cells that have activated p*SYN1*; nv (no virus), no infection was performed. Cells analyzed (A–C, E, and F) or the number of cells showing PSCs from tested cells (H and I) are indicated above bars.

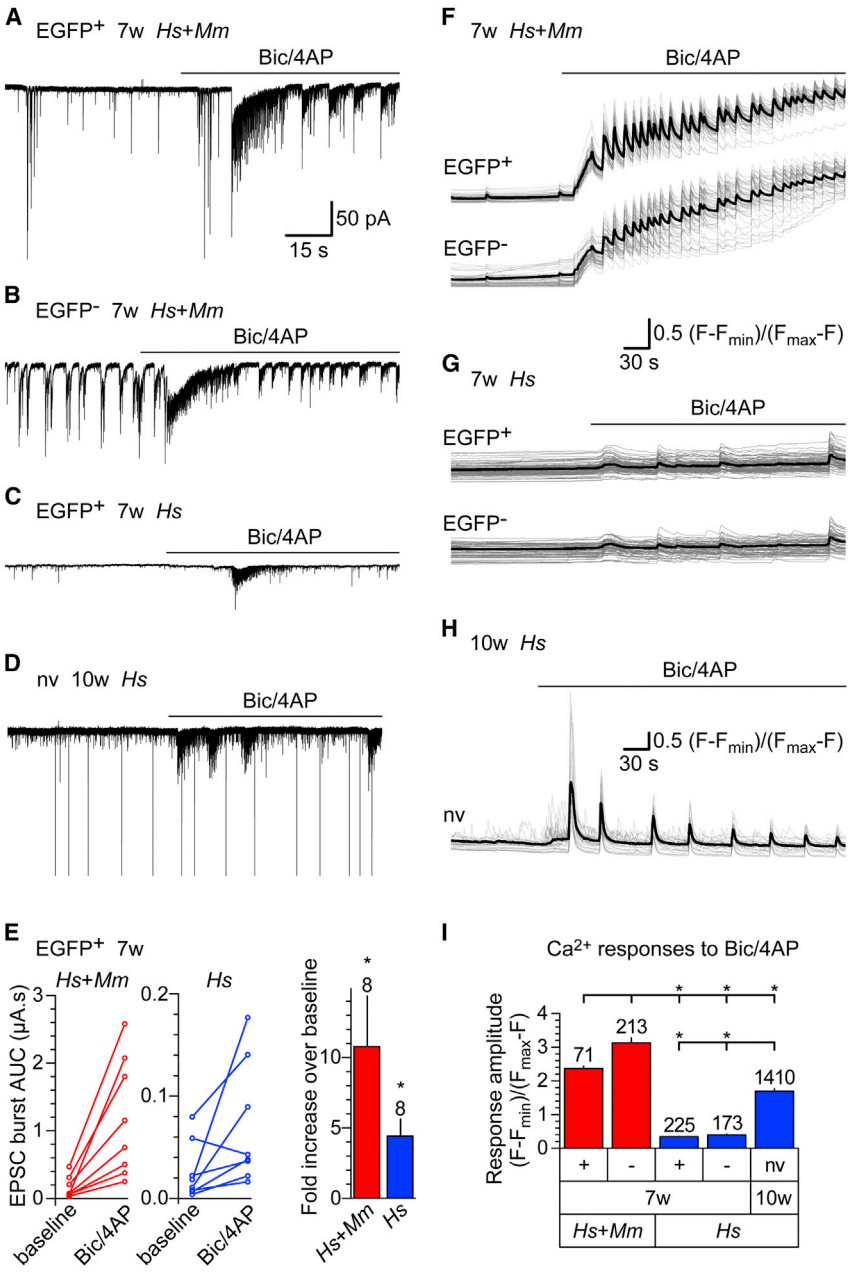

Figure 2. Induction of Synaptic Activity and Somatic Ca^{2+} Signals in hiPSCd Neurons

All culture conditions and cell groups analyzed are specified at the end of the figure legend.

(A–D) Traces of responses to bicuculline and 4-aminopyridine (Bic/4AP, 50 µM and 250 µM, respectively) at Vhold = −70 mV are shown in an EGFP positive (A) and an EGFP negative (B) cell of a 7-week mixed-species culture, and in an EGFP positive cell of a 7-week hiPSCd neuron-only culture (C) and in a cell of a 10-week hiPSCd neuron-only culture not exposed to virus (D).

(E) Area under the curve (AUC) from integrals of currents measured in human cells over equal time periods before (baseline) and after the application of Bic/4AP. Line series plots connect the values from each cell measured, and the bar graph shows the increase in excitatory postsynaptic current (EPSC) burst AUC (mean ± SEM). Cell numbers are specified above bars. Two-tailed Student's t test, $^*p < 0.05$.

(F–H) Traces of Rhod2 Ca^{2+} imaging with responses to Bic/4AP in EGFP positive and negative cells of a 7-week mixed-species culture (F) and a hiPSCd neuron-only culture (G), and in cells of a 10-week hiPSCd neuron-only culture not exposed to virus (H). Gray lines represent individual cells and black lines are the averages.

(I) Bic/4AP-induced Ca^{2+} response amplitudes (peak minus baseline, mean ± SEM). Cell numbers are specified above bars. Two-way ANOVA on ranks and Holm-Sidak test, $^*p < 0.05$.

Hs + *Mm*, mixed-species culture; *Hs*, hiPSCd neuron-only culture; 7w or 10w, human NPCs were differentiated for 7 or 10 weeks, respectively. Human cells were infected with a lentivirus encoding EGFP under the control of p*SYN1* or not infected (no virus, nv). + and $EGFP^+$ or − and $EGFP^-$ denote cells that express or do not express lentivirus-encoded EGFP, respectively.

neuron-only cultures, the induction of *NPAS4* and *FOS* was severely reduced in the presence of TTX, Nif, APV/MK, or Nif/APV/MK, although the effect of Nif on *FOS* was comparatively weaker (Figure 3F). *ARC* induction was reduced by blocking VGCCs and/or NMDA receptors in both cultures (Figures 3E and 3F). Finally, co-culture experiments with hiPSCd neurons produced from a distinct iPSC line (hiPS 3, see the Experimental Procedures) produced nearly identical results (Figures S2B and S2C).

To determine the proportion of hiPSCd neurons responding to Bic/4AP treatment with IE gene induction and to confirm the response at the protein level, we used immunostaining for yet another classical IE gene product, JUNB. Approximately 65% of hiPSCd neurons in the co-culture showed JUNB protein expression after 2 hr of enhanced excitatory synaptic input (Figure 3G).

These results demonstrate that strong induction of excitatory synaptic activity-dependent IE gene expression in human cells can be evoked by a simple Bic/4AP treatment of hiPSCd cultures. Also, they show that NMDA receptors and VGCCs are involved in triggering synaptic activity-induced increases in IE gene mRNA levels in hiPSCd neurons.

Early Gene Expression Response to Synaptic Activity Is Generic but Has Lineage-Specific Features

We performed RNA-seq to examine the synaptic activity-regulated gene program in hiPSCd neurons. RNA levels of 50 or 42 human genes were significantly changed (Benjamini-Hochberg adjusted p [p_{adj}] < 0.1) in hiPSCd neurons 1 hr after Bic/4AP addition to the 7-week mixed-species cultures (Figure 4A; Table S2) or to the 10-week hiPSCd neuron cultures (Table S2),

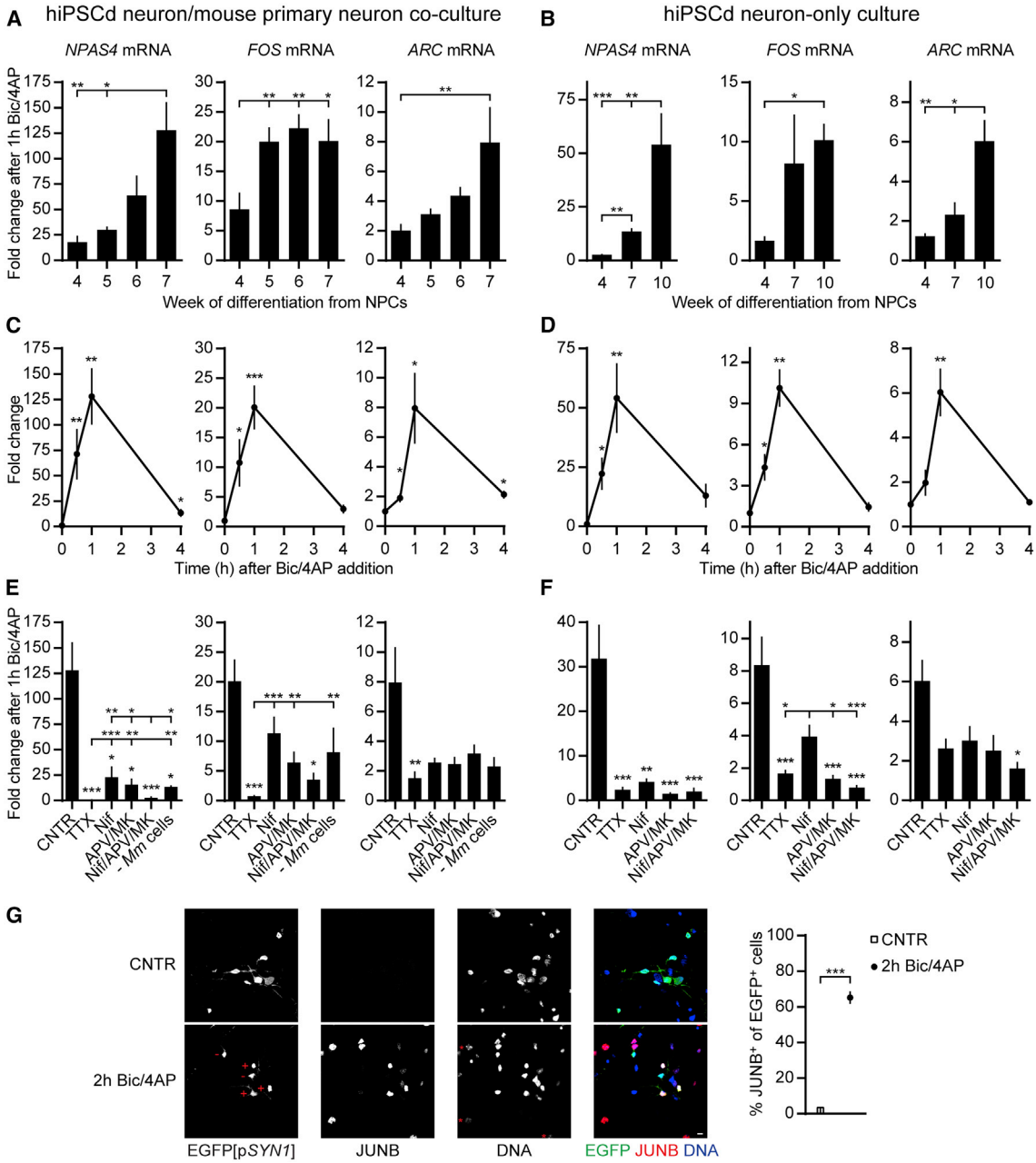

Figure 3. Excitatory Synaptic Input to hiPSCd Neurons Upregulates Human Immediate-Early Genes

(A–F) RT-qPCR analysis of human *NPAS4*, *FOS*, and *ARC* mRNA levels after treatment of hiPSCd neuron/mouse primary hippocampal neuron co-cultures (A, C, and E) or hiPSCd neuron-only cultures (B, D, and F) with bicuculline and 4-aminopyridine (Bic/4AP, 50 μM/250 μM).

(A and B) Impact of duration of hiPSCd neuron differentiation on IE gene induction is shown.

(C and D) Temporal profiles of IE gene mRNA levels in response to Bic/4AP treatment are shown. 7-week (C) or 10-week (D) cultures.

(E and F) Effects of blocking action potentials (TTX, tetrodotoxin; 1 μM), VGCCs (Nif, Nifedipine; 10 μM), or NMDA receptors (APV/MK, 2-amino-5-phosphonovalerate, 50 μM and MK801, 10 μM), or both VGCCs and NMDA receptors (Nif/APV/MK), on the induction of IE genes in response to Bic/4AP treatment. 7-week (E) or 10-week (F) cultures. Results with the 7-week hiPSCd neuron cultures without mouse neurons are also shown (E, – *Mm* cells).

(G) Immunofluorescence staining of the 7-week co-culture for JUNB expression before (CNTR) or after treatment with Bic/4AP for 2 hr (2h Bic/4AP). EGFP expression (direct fluorescence) under the control of the human *SYN1* promoter (EGFP[p*SYN1*], lentiviral infection of NPCs) identifies human neurons. DNA, Hoechst stain. Red + or – indicates a $JUNB^+$ or $JUNB^-$ hiPSCd neuron, respectively. Red asterisks mark presumable mouse neurons with distinctive Hoechst staining. Confocal images scale bar, 10 μm.

n = 3–8 (A and G), n = 3–4 (C and E), or n = 3 (B, D, and F); mean ± SEM; (A, B, E, and F) one-way ANOVA and Tukey's test; (C, D, and G) two-tailed Welch's t tests; *p < 0.05, **p < 0.01, and ***p < 0.001. If not specified with lines, the asterisks indicate significance compared to control. See also Figures S2B and S2C.

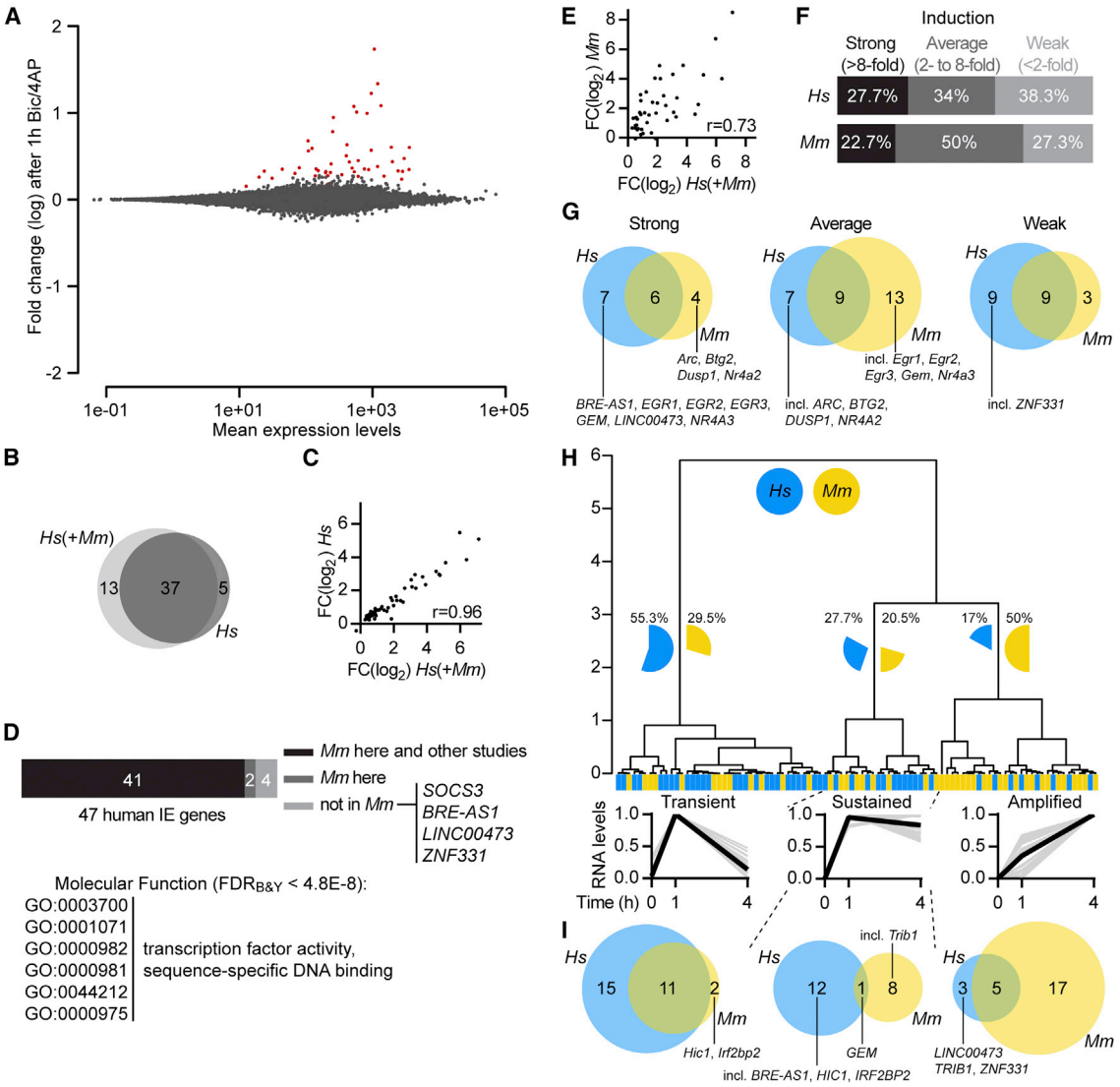

Figure 4. Generic Early Response to Synaptic Activity with Species-Specific Features in hiPSCd Neurons

(A) Gene expression log ratio versus expression level average (MA) plot of gene expression changes detected with RNA-Seq in hiPSCd neurons 1 hr after Bic/4AP addition to the 7-week mixed-species cultures. Dots representing genes with significantly changed RNA levels ($p_{adj} < 0.1$) are red. n = 4.

(B) Venn diagram displays human genes with significantly changed RNA levels after 1-hr Bic/4AP treatment of 7-week mixed-species cultures (*Hs*[+*Mm*]) and 10-week hiPSCd neuron cultures (*Hs*).

(C) Correlation of expression $\log_2$ fold change (FC[$\log_2$]) values of all of the 55 human genes shown in (B) in the *Hs*(+*Mm*) culture with the respective values obtained from the *Hs* culture. Dots represent mean values of four biological replicate experiments. Pearson's r, $p < 0.0001$.

(D) Distribution of activity-regulated human IE genes according to the information on their mouse orthologs. *Mm* here and other studies, genes whose mouse orthologs' RNA levels are changed in this and other studies; *Mm* here, genes whose mouse orthologs' mRNA levels are changed only in this study; and not in *Mm*, no evidence for neuronal activity-dependent regulation of the mouse ortholog (*SOCS3*) or no ortholog in mouse. The most enriched GO terms within the human IE genes are shown.

(E) Correlation of expression FC($\log_2$) values of 47 human IE genes in the mixed-species culture after 1 hr of Bic/4AP treatment with the FC($\log_2$) values of their mouse orthologs in the same culture. Dots represent the mean values of four biological replicate experiments. Pearson's r, $p < 0.0001$.

(F) Distribution of human IE genes and their mouse orthologs based on induction strength in hiPSCd neurons and mouse neurons, respectively, in the co-culture is shown.

(G) Venn diagrams display strongly, averagely, or weakly induced human (*Hs*) IE genes and their mouse (*Mm*) orthologs after 1 hr of Bic/4AP treatment of the mixed-species culture.

(H) Hierarchical clustering of human (*Hs*) IE genes and their mouse (*Mm*) orthologs according to temporal expression profiles after the induction of synaptic activity in the co-culture. Blue and yellow rectangles denote human and mouse genes, respectively. Expression profiles in three clusters evident at dendrogram height 3 are depicted below the dendrogram. Gray lines show single genes and black lines are the averages.

(I) Venn diagrams display transient, sustained, and amplified human (*Hs*) IE genes and their mouse (*Mm*) orthologs.

See also Figures S3–S5.

respectively. RNA levels of 37 human genes were significantly changed in both culture systems (Figure 4B). The expression fold change values of all of the obtained 55 genes between the two cultures were nearly equivalent (Pearson's r [r] = 0.96; Figure 4C), supporting the validity of the mixed-species RNA-seq analysis (see the Supplemental Experimental Procedures). We assigned a human gene to be a putative IE gene (hereafter IE gene) if the significant expression level change ($p_{adj} < 0.1$) in one dataset was supported by a change with an unadjusted p less than 0.01 in the other or if the change was more than 2-fold with the p_{adj} less than 0.05 in at least one of the datasets. Altogether we identified 47 human synaptic activity-regulated IE genes, all with upregulated RNA levels (Table S3). RNA-seq results with the mixed-species samples were validated for hiPSCd neurons derived from two different iPSC lines with the nCounter method using species-specific probes (Figures S2D and S3–S5).

We categorized the 47 human IE genes according to the data available for their rodent orthologs (Figure 4D). The rodent orthologs of 41 of the human IE genes (87.2%) were significantly upregulated after Bic/4AP treatment in mouse primary neurons according to our RNA-seq and nCounter analysis, and they have been reported to be neuronal activity regulated in other studies using different experimental systems and time points (Kim et al., 2010; Maze et al., 2015; Rossner et al., 1997; Saha et al., 2011; Spiegel et al., 2014; Zhang et al., 2007, 2009). The orthologs of three human IE genes (*C11orf96*, *MIR22HG*, and *SOCS3*) have not been previously identified as activity-regulated genes in rodents, although *SOCS3* was only regulated in one of the two iPSC lines used here. Three of the human IE genes, *BRE-AS1*, *LINC00473*, and *ZNF331*, are exceptional because they do not have rodent orthologs. *BRE-AS1* and *LINC00473* RNA levels were detected to be strongly (≥15-fold) and *ZNF331* RNA levels weakly (1.5-fold) upregulated in hiPSCd neurons with RNA-seq after 1 hr of Bic/4AP treatment, and all three genes were confirmed to be activity induced with nCounter analysis in hiPSCd neurons derived from both of the iPSC lines used here (Figures S3 and S5). Also, their synaptic activity-induced expression was blocked or severely reduced in the presence of TTX or Nif/APV/MK (Figure S2D). *BRE-AS1* is a noncoding RNA gene antisense to the *BRE* (*brain and reproductive organ-expressed*) gene. *LINC00473* is a primate-specific long noncoding RNA gene that has been documented to be duplicated along with only three other genes in a patient with delayed speech and language development (DECIPHER 277616; Firth et al., 2009). *ZNF331* encodes a Krüppel-associated box domain-containing transcriptional repressor.

The most significantly over-represented gene ontology (GO) terms among the human synaptic activity-regulated IE genes were all associated with transcription factor activity (Figure 4D; Table S4; 24 genes, 51.1%, encode transcription factors). Also, cAMP response elements (CREs) or CRE half site (CREhs)-containing sequences and serum response elements (SREs) were significantly enriched in the proximal promoter regions of human IE genes (Table S4), suggesting that many of them are targets of the well-established neuronal activity-dependent transcriptional regulators, CRE-binding protein (CREB) and SRE-interacting proteins (Bading et al., 1993).

Next, we compared the synaptic activity-regulated human IE genes to their mouse orthologs using the data from the co-cultures where RNA of the two species is collected from cells stimulated in identical culture conditions. Rapid human RNA level changes after enhancement of glutamatergic synaptic activity were paralleled by similar changes of the respective mouse orthologs (Figure 4E; expression change correlation, r = 0.73). Based on induction strength, half of the IE gene ortholog pairs grouped together (Figures 4F and 4G). For example, *EGR4*/*Egr4*, *FOS*/*Fos*, *FOSB*/*Fosb*, *JUNB*/*Junb*, *NPAS4*/*Npas4*, and *NR4A1*/*Nr4a1* were strongly induced in human cells as well as in mouse cells. To classify genes in terms of temporal expression profile regardless of induction strength, we performed hierarchical clustering of human IE genes together with their mouse orthologs, if present, based on RNA levels scaled between 0 and 1 from untreated and 1- or 4-hr Bic/4AP-treated mixed-species cultures (Figure 4H). Relative to their upregulated expression levels at the 1-hr time point, IE gene RNA levels at the 4-hr time point were either decreased (termed here transient), unchanged (termed sustained), or further increased (termed amplified). This analysis revealed that half of the examined mouse genes, but only 17% of the human IE genes, belonged to the amplified cluster. Instead, 55.3% of the human IE genes grouped into the transient set of genes and 27.7% had the sustained RNA expression profile. Examples of transient human IE genes with amplified or sustained mouse orthologs include *GADD45B*/*Gadd45b* and *NR4A2*/*Nr4a2* or *FOSB*/*Fosb* and *NPAS4*/*Npas4*, respectively. Human *HIC1*, encoding *hypermethylated in cancer 1*, grouped to the sustained cluster and mouse *Hic1* grouped to the transient cluster. *HIC1*/*Hic1* is the only relatively strongly induced IE gene in both cell types (human, 5.9-fold; mouse, 4.5-fold) that had a more sustained increase in expression levels in hiPSCd neurons compared to mouse neurons (Figure 4I). These results establish that overall the hiPSCd neuron synaptic activity-responsive IE gene program is generic. However, it involves genes that do not have orthologs in the mouse, and many of the human IE genes are in hiPSCd neurons upregulated more transiently than their mouse orthologs in mouse primary hippocampal neurons.

Conserved Ca^{2+}-Signaling Pathway Regulates *BRE-AS1*, *LINC00473*, and *ZNF331* Promoters

We next asked if the three synaptic activity-regulated human IE genes that do not have mouse orthologs (see Figure 5A for nCounter confirmation of RNA-seq results) represent loci regulated by neuronal activity via conserved mechanisms or are induced by cell-type or species-specific mechanisms. To answer this, we conducted luciferase reporter assays for the regulation of *BRE-AS1*, *LINC00473*, and *ZNF331* promoters in mouse primary hippocampal and cortical neurons. The promoters of these genes contain CRE and CREhs *cis* elements (Figure 5B) that may direct the induction of promoter activity upon excitatory synaptic signaling, and, moreover, the *LINC00473* promoter (p*LINC00473*) contains a bHLH-PAS transcription factor response element (PasRE; Figure 5B) that could permit the enhancement of transcriptional activity after the immediate response. The assays showed increases in normalized luciferase levels 6 hr after Bic/4AP addition with the *BRE-AS1* promoter (p*BRE-AS1*) and p*LINC00473* and two of the cloned *ZNF331* promoter-containing regions (p*ZNF331* II and

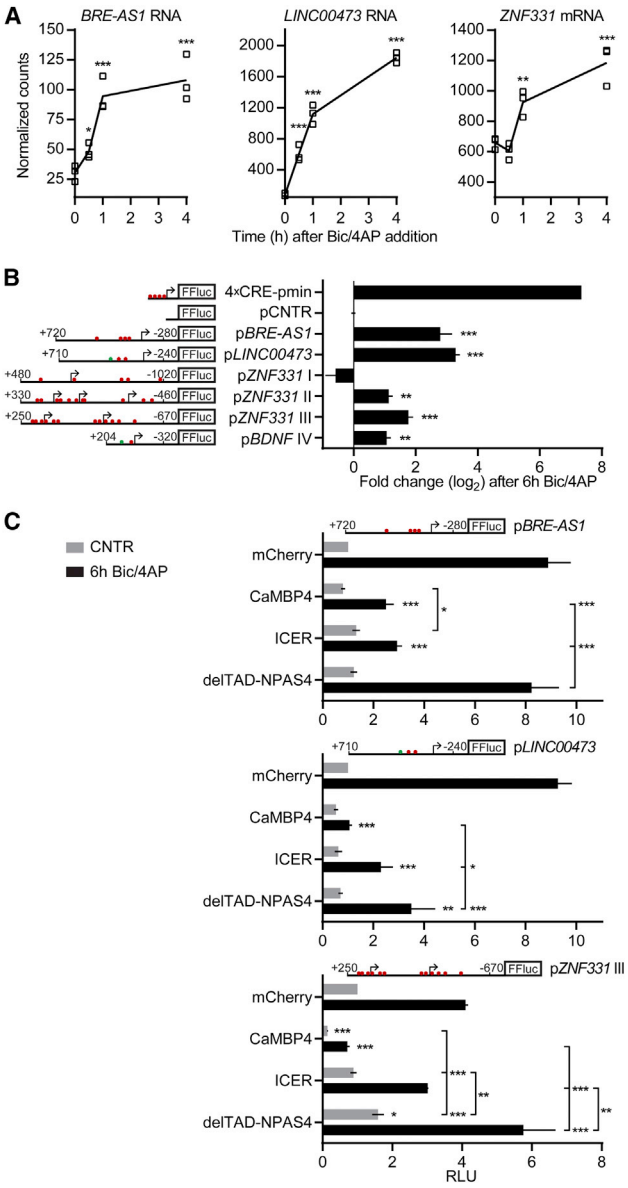

Figure 5. *BRE-AS1*, *LINC00473*, and *ZNF331* Regulation by Conserved Ca^{2+}-Signaling Pathway

(A) Results of nCounter analyses of *BRE-AS1*, *LINC00473*, and *ZNF331* expression in response to Bic/4AP treatment of 7-week mixed-species cultures are shown.

(B and C) Luciferase reporter assays with the firefly luciferase (FFluc) under the control of the indicated promoter or without a promoter (pCNTR) in mouse primary hippocampal neurons.

(B) Change in FFluc activity in response to Bic/4AP treatment. See also Figure S6A.

(C) Relative light units (RLUs) measured from untreated cells (CNTR) or cells treated 6 hr with Bic/4AP (6h Bic/4AP). The protein encoded by the co-transfected plasmid is shown on the left.

Arrows denote transcription start sites (TSSs). Numbers specify base pairs upstream (−) or downstream (+) of the most 5′ or 3′ TSS, respectively. Red or green dots represent CRE and CREhs or PasRE *cis* elements, respectively.

n = 3 (A–C); (A) independent measurements and mean; (B and C) mean ± SEM; (A and B) one-way ANOVA and Dunnett's test; (C) two-way ANOVA and Tukey's test; *p < 0.05, **p < 0.01, and ***p < 0.001. If not specified with lines, the asterisks indicate significance compared to untreated control (A), to pCNTR (B), or to cells expressing mCherry in the same treatment group (CNTR or 6h Bic/4AP) (C).

III, covering three and two 5′ exons, respectively; Figures 5B and S6A). These results reveal that *BRE-AS1*, *LINC00473*, and *ZNF331* are under the control of promoters that are responsive to synaptic activity in mouse neurons. This demonstrates that they are targets of evolutionarily conserved synapse-to-nucleus signaling mechanisms, most probably involving nuclear Ca^{2+}/calmodulin kinases (Bading, 2013).

To investigate if synaptic activity-dependent regulation of p*BRE-AS1*, p*LINC00473*, and p*ZNF331* III is sensitive to nuclear Ca^{2+}/calmodulin inhibition and interference with CRE-dependent or PasRE-mediated transcription, we used co-transfection of constructs encoding for one of the following proteins: (1) CaMBP4, a nuclear-localized inhibitor of Ca^{2+}/calmodulin signaling (Wang et al., 1995; Zhang et al., 2007); (2) ICER1 (ICER), an inhibitor of CREB family proteins (De Cesare and Sassone-Corsi, 2000); or (3) NPAS4 without the transcription activation domain (delTAD-NPAS4), a dominant-negative regulator of bHLH-PAS transcription factors (Pruunsild et al., 2011). We found that luciferase expression under the control of p*BRE-AS1*, p*LINC00473*, and p*ZNF331* III after 6 hr of Bic/4AP treatment was significantly reduced by CaMBP4 (Figure 5C). Overexpression of ICER led to diminished Bic/4AP-induced luciferase levels with p*BRE-AS1* and p*LINC00473*, but not with p*ZNF331* III. The dominant-negative bHLH-PAS factor delTAD-NPAS4 considerably lowered Bic/4AP-induced transcription only from p*LINC00473* (Figure 5C). Additionally, p*ZNF331* III activity was significantly reduced by CaMBP4 in unstimulated conditions, indicating that basal nuclear Ca^{2+}/calmodulin activity regulates transcription from this promoter. Collectively, these results prove that the promoters of human *BRE-AS1*, *LINC00473*, and the most 3′ promoter-containing region of *ZNF331* are regulated by the conserved Ca^{2+}-signaling pathway that activates nuclear Ca^{2+}/calmodulin kinases in neurons. p*BRE-AS1* and p*LINC00473* are probably induced by CREB, and the transcriptional activity from p*LINC00473* is likely to be increased by recruitment of the bHLH-PAS transcription factor NPAS4 and ARNT2 heterodimer to the PasRE.

hiPSCd Neuron Synaptic Activity-Controlled Late Response Gene Set Contains Cell Type-Specifically Regulated Genes

RNA levels of 428 or 215 human genes were detected to be significantly changed ($p_{adj} < 0.1$) with RNA-seq 4 hr after Bic/4AP addition to the 7-week hiPSCd neuron/mouse primary hippocampal neuron co-culture (Figure 6A; Table S5) or to the 10-week hiPSCd neuron-only culture (Table S5), respectively. Although the overlap of significantly regulated genes was smaller between the two culture conditions than detected for the 1-hr time point (Figures 6B and 4B), the mean fold change values of the total of these 524 genes correlated strongly between the datasets (Figure 6C, r = 0.88). Using the same two criteria as for defining the human IE genes, we designated 218 human genes to belong to the later phase of the synaptic activity-responsive

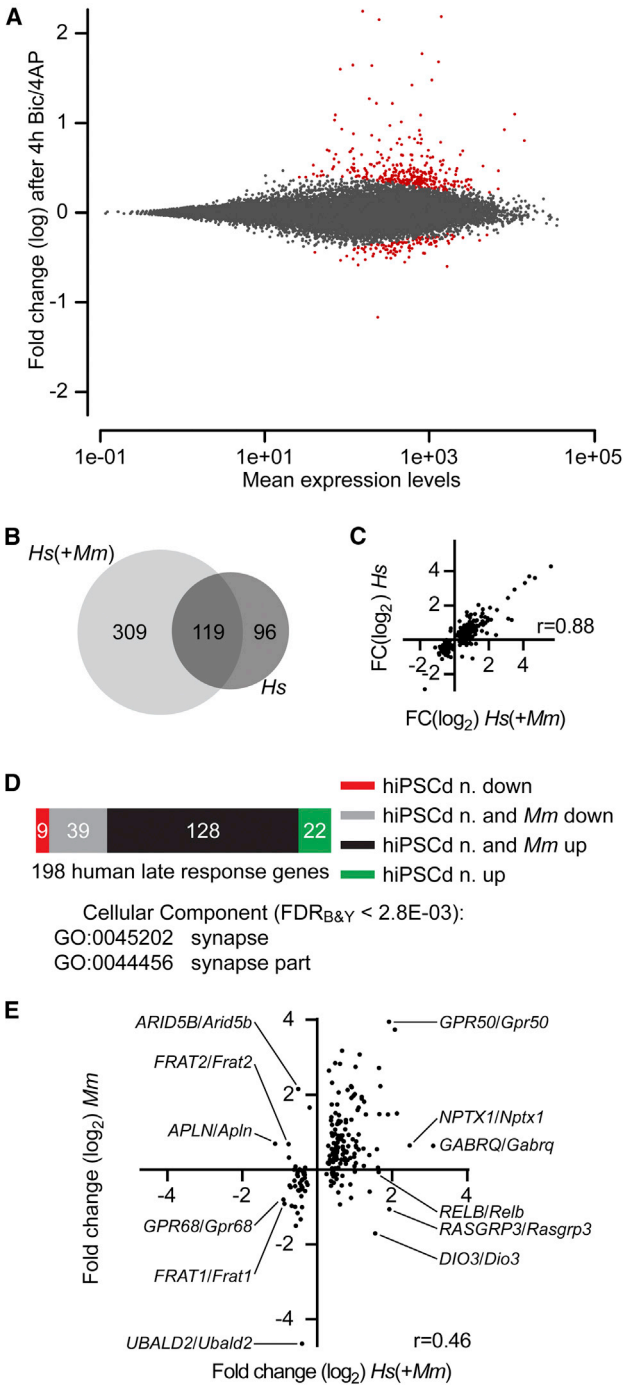

Figure 6. Human iPSCd Neuron Synaptic Activity-Regulated Late-Response Genes

(A) RNA-seq MA plot of gene expression changes in hiPSCd neurons 4 hr after Bic/4AP addition to the 7-week mixed-species cultures. Dots representing genes with significantly changed RNA levels ($p_{adj} < 0.1$) are red. n = 3.

(B) Venn diagram displays human genes with significantly changed RNA levels after 4-hr Bic/4AP treatment of 7-week mixed-species cultures (*Hs*[+*Mm*]) and 10-week hiPSCd neuron cultures (*Hs*).

(C) Correlation of expression $\log_2$ fold change (FC[log2]) values of all of the 524 human genes shown in (B) in *Hs*(+*Mm*) culture with the respective values obtained from the *Hs* culture. Dots represent mean values of three biological replicate experiments. Pearson's r, $p < 0.0001$.

(D) Distribution of the human late-response (LR) genes according to the information on their mouse orthologs. hiPSCd n. down, downregulated in hiPSCd neurons but no evidence for neuronal activity-dependent downregulation of the mouse ortholog or no mouse ortholog; hiPSCd n. and *Mm* down, downregulated in hiPSCd neurons and the mouse ortholog downregulated in this and/or other studies; hiPSCd n. and *Mm* up, upregulated in hiPSCd neurons and the mouse ortholog upregulated in this and/or other studies; and hiPSCd n. up, upregulated in hiPSCd neurons but no evidence for neuronal activity-dependent upregulation of the mouse ortholog. See also Table S7. GO terms enriched within upregulated human LR genes are shown.

(E) Correlation of expression FC($\log_2$) values of 198 human LR genes in the co-culture after 4 hr of Bic/4AP treatment with the FC($\log_2$) values of their mouse orthologs in the same culture. Dots represent mean values of three biological replicate experiments. Examples that are among the most strongly up- or downregulated genes in either of the species are indicated. Pearson's r, $p < 0.0001$.

See also Figures S3–S5.

genomic program in hiPSCd neurons. From these we excluded 20 genes that we had designated to be IE genes, and we acquired a set of 198 human synaptic activity-regulated late-response (LR) genes (Table S6; Figure 6D). The majority of the human LR genes (167 genes, 84.3%) have mouse orthologs that were correspondingly regulated in mouse primary neurons in this study and/or have been shown previously to be activity regulated (Balik et al., 2013; Kim et al., 2010; Maze et al., 2015; Mo et al., 2015; Saha et al., 2011; Spiegel et al., 2014; Zanzouri et al., 2006; Zhang et al., 2007, 2009). The mouse orthologs of 22 or nine human LR genes that were up- or downregulated, respectively, in hiPSCd neurons have not been described to be neuronal activity regulated or have been found to be regulated in the opposite direction in mice by others and/or by us (Table S7).

The only significantly enriched GO categories among the 150 upregulated human LR genes were synapse (GO:0045202, false discovery rate $[FDR]_{B\&Y}$ = 2.56E−03) and synapse part (GO:0044456, $FDR_{B\&Y}$ = 2.74E−03, Figure 6D). This suggests that a key consequence of synaptic activity-dependent gene expression in hiPSCd neurons could be the adjustment of the composition and function of synapses. Downregulated genes did not have significant over-representation of any GO term.

RNA level changes of the human LR genes and their mouse orthologs in the 7-week mixed-species cultures were positively correlated (r = 0.46; Figure 6E). However, the correlation between human and mouse gene RNA level changes 4 hr after the Bic/4AP addition was significantly weaker than that at the 1-hr time point (r = 0.46 versus r = 0.73, Z = 2.5, p = 0.012, Fisher Z-transformation). Furthermore, the levels of a number of human LR genes were changed hiPSCd neuron specifically, suggesting that the late phase of the transcriptional response to synaptic activity depends more on the cell type and/or the species than the early phase. We also noted that the human LR genes include the orthologs for 26 mouse excitatory neuron-specifically induced genes, like *Erf*, *Homer1*, and *Scg2*, and ten mouse inhibitory neuron-specifically induced genes, like *Nab1* and *Hivep2* (Spiegel et al., 2014), indicating that the activity-regulated gene program described here for hiPSCd neurons originates from

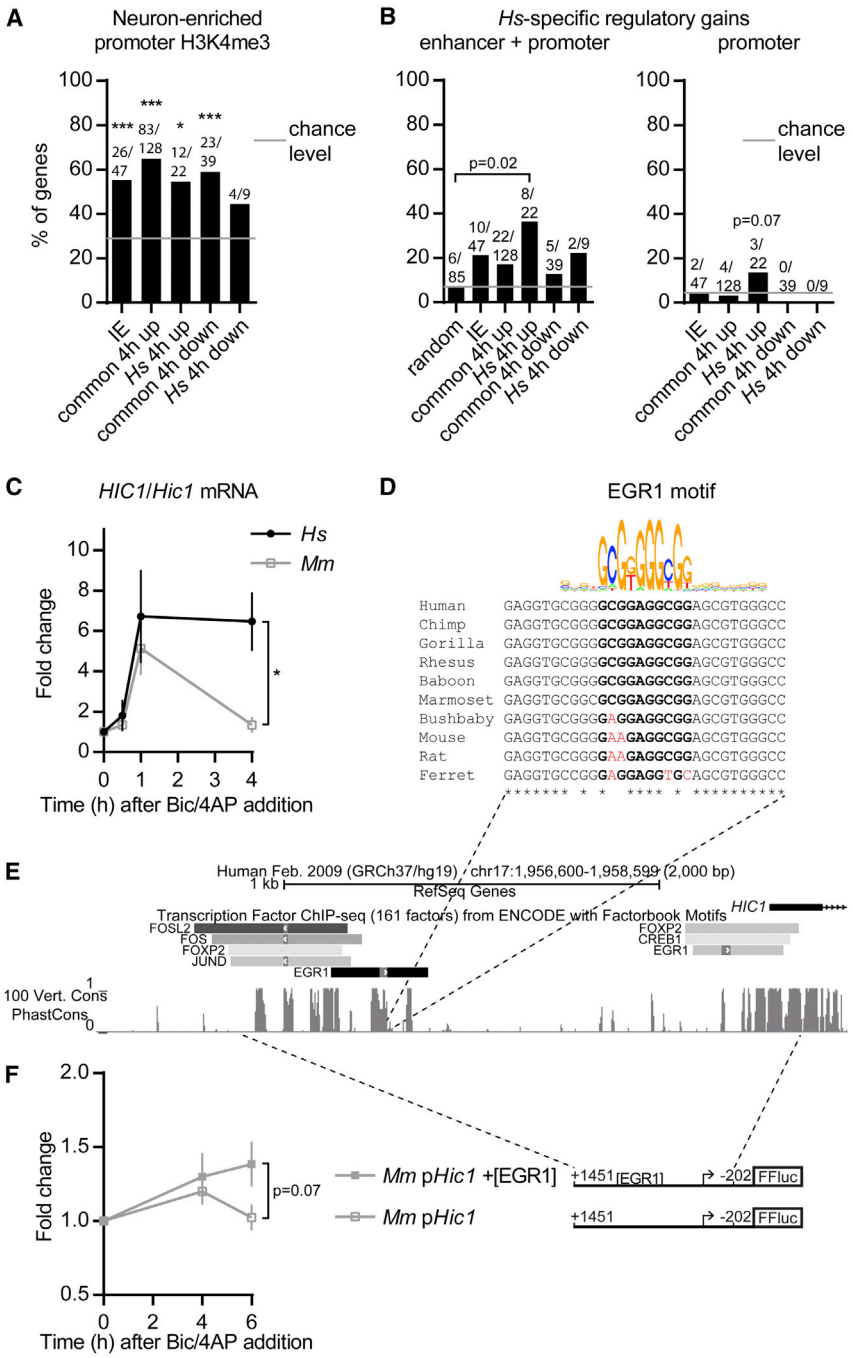

Figure 7. Potential Species-Specific Control of hiPSCd Neuron Synaptic Activity-Regulated Genes

(A) Percentages of human synaptic activity-regulated IE or LR genes positive for neuron-enriched promoter H3K4me3 mark, according to the data from Cheung et al. (2010), are shown.

(B) Percentages of human synaptic activity-regulated IE or LR genes positive for human-specific (*Hs*-specific) epigenetic enhancer and/or promoter regulatory gain(s), according to the data from Reilly et al. (2015), are shown.

(A and B) LR genes were grouped as per Figure 6D. Common, regulation in hiPSCd neurons and in mouse; *Hs*, regulation only in hiPSCd neurons; random, random genes from all genes assessed by RNA-seq. Numbers above bars specify genes with the respective epigenetic modification from genes in each group. (A and promoter gains in B) Binominal test, *p < 0.05 and ***p < 0.001. Enhancer + promoter gains in (B), Holm adjusted Fisher's exact test.

(C) RT-qPCR analysis of human (*Hs*) and mouse (*Mm*) *HIC1*/*Hic1* mRNA levels after treatment of the mixed-species culture with Bic/4AP. n = 3; mean ± SEM; Holm-Sidak adjusted t tests, asterisk indicates significance at 4 hr, *p < 0.05. See also Figure S6B.

(D) Ten-species multiple alignment of a part of the conserved sequence element containing the EGR1-binding motif in the human *HIC1* promoter is shown.

(E) Conservation (100 vertebrate species phastCons) of the human *HIC1* promoter adapted from the University of California, Santa Cruz (UCSC) Genome Browser with the ENCODE project transcription factor-binding sites determined with ChIP-seq for the indicated transcription factors is shown.

(F) Luciferase reporter assay with the firefly luciferase (FFluc) under the control of the mouse *Hic1* promoter in mouse primary hippocampal neurons. Response to Bic/4AP treatment is shown. TSSs are indicated with arrows. Numbers specify base pairs upstream (−) or downstream (+) of the TSS. [+EGR1], addition of the EGR1 site shown in (D) by mutation of two nucleotides according to the human sequence. n = 3; mean ± SEM; Holm-Sidak adjusted t tests, p value is for the 6-hr time point.

both excitatory and inhibitory cells. It seems likely that the neuron type, including possible effects determined by the species, defines the complete set of LR genes that are regulated by synaptic activity.

Potential Lineage-Specific Control of Synaptic Activity-Regulated Genes

It is uncertain whether synaptic activity-induced transcription in hiPSCd neurons reflects that of the human brain in vivo. Testing this experimentally in humans is inconceivable, so we addressed the question indirectly. First, we used the dataset from Cheung et al. (2010) to find out if the promoters of human genes regulated by synaptic activity in hiPSCd neurons have a neuron-enriched open chromatin-associated transcription initiation mark H3K4me3 in the human prefrontal cortex in vivo during development and in the adult. This is indicative of the genes' accessibility for activity-dependent regulation in the human brain in vivo. The neuron-enriched H3K4me3 promoter mark was present on significantly more genes than expected by chance in all hiPSCd neuron synaptic activity-regulated gene groups, except the hiPSCd neuron-specifically downregulated genes (Figure 7A). This reveals that the genes detected here to be synaptic activity regulated in hiPSCd neurons are enriched for genes that are more apt to transcription in the human brain than in other tissues.

We next explored whether the synaptic activity-controlled gene program described here includes human genes associated with regulatory changes compared to other mammals, by examining if hiPSCd neuron activity-regulated genes have human-specific promoter or enhancer H3K27ac and/or H3K4me2 gains during human brain cortex development in vivo, according to the data from Reilly et al. (2015). Significantly more genes than expected by chance were positive for a human-specific epigenetic regulatory gain only among the genes that were hiPSCd neuron-specifically upregulated by 4 hr of Bic/4AP-induced activity (Figure 7B). This infers that expression of a relatively large proportion of the genes shown here to be responsive to synaptic activity only in hiPSCd neurons is probably regulated in a human-specific manner also in the brain in vivo.

Finally, we focused on *HIC1*/*Hic1* to study if regulatory DNA sequence dissimilarities of species rather than the cell type could explain temporal differences in gene expression in response to synaptic activity between hiPSCd neurons and mouse primary neurons. We chose *HIC1*/*Hic1* because it was the only relatively strongly induced IE gene that was upregulated more transiently in mouse neurons compared to hiPSCd neurons, a result that we confirmed with species-specific RT-qPCR (Figures 7C and S6B). The promoter of *HIC1*/*Hic1* is not well conserved among vertebrates in general, but it contains several almost identical regions potentially encompassing important regulatory sequences (Figure 7E). We searched these conserved sequences for *cis* elements that are bound by transcription factors in human cells using the Encyclopedia of DNA Elements (ENCODE) chromatin immunoprecipitation sequencing (ChIP-seq) data, and we found that the only orthologous binding motif relevant to activity-controlled gene regulation that is not present in the rodent *Hic1* promoter is the IE protein EGR1-binding sequence located ~1,000 bp upstream of the human *HIC1* RefSeq transcript 5′ end (Figures 7D and 7E). This suggests that, upon synaptic activity, mRNA levels of mouse *Hic1* may not be sustained because Egr1 cannot bind to the mouse *Hic1* promoter. To test this, we generated a luciferase reporter construct with the mouse *Hic1* promoter, and, for comparison, we inserted the EGR1 site in it by changing two nucleotides according to the human *HIC1* promoter. Consistent with our hypothesis, luciferase assays in mouse primary neurons revealed that the mouse *Hic1* promoter humanized with the EGR1 motif produced a moderate rise in luciferase levels after 6 hr of Bic/4AP treatment, whereas the wild-type promoter did not (Figure 7F). This result supports the idea that a simple DNA element alteration in the promoter could lead to a difference in the temporal profile of *Hic1* expression in response to synaptic activity in mice compared to its ortholog's expression profile in humans.

DISCUSSION

This study reveals three ways in which the human genetic background influences neuronal adaptogenomics compared to that of mice: (1) it expands the repertoire of human synaptic activity-regulated genes with lineage-specific genes, (2) it permits synaptic activity-dependent regulation of some human genes whose orthologs are not activity-regulated in mice, and (3) it can gene-selectively change the temporal profile of synaptic activity-responsive transcriptional activity.

We identify three human genes, *BRE-AS1*, *LINC00473*, and *ZNF331*, that lack mouse orthologs but are regulated by synaptic activity via conserved signaling mechanisms to be included in the human activity-responsive adaptive gene program. *LINC00473*, which belongs to the core set of hiPSCd neuron synaptic activity-regulated genes (Figure S7), has been shown to be a primate-specific cAMP pathway-responsive noncoding RNA that negatively regulates IE genes (Reitmair et al., 2012). *ZNF331* and also *HIC1*/*Hic1*, the only relatively strongly induced IE gene that had a more sustained induction in humans compared to mice, encode transcriptional repressors. Interestingly, a number of synaptic activity-controlled IE genes were upregulated more transiently in hiPSCd neurons than their mouse counterparts in primary neurons (e.g., *EGR4*/*Egr4*, *FOSB*/*Fosb*, and *NPAS4*/*Npas4*), possibly reflecting lineage-specific IE gene regulation by *LINC00473*, *ZNF331*, and *HIC1*. More transient upregulation of some of the IE genes in hiPSCd neurons cannot be explained by a lack of sustained Bic/4AP-induced activity and mechanisms amplifying transcription, since the distinct temporal regulation of synaptic activity-controlled genes between hiPSCd neurons and mouse primary neurons was gene selective. Specifically, along with the distinct temporal profiles, the upregulation of several orthologous IE genes in both human and mouse cells was commonly transient (e.g., *ARC*/*Arc*, *BTG2*/*Btg2*, and *NR4A1*/*Nr4a1*) or commonly amplified after the initial response (e.g., *CSRNP1*/*Csrnp1*, *FOSL2*/*Fosl2*, and *RGS2*/*Rgs2*). We therefore propose that genetic differences gene-selectively cause some of the orthologous human and mouse IE genes to have different expression kinetics after synaptic activity. The mechanisms probably involve both regulation in *trans*, including regulation by lineage-specific activity-responsive genes as discussed above, and regulation in *cis*, as indicated by our result with the *Hic1* promoter that suggests a role for a species-specific *cis*-regulatory element. Such an interpretation also is supported by a recent study that used a high concentration of extracellular KCl to stimulate neurons (Qiu et al., 2016).

In rodents a large fraction of neuronal activity-induced IE genes are transcription factors (Lanahan and Worley, 1998). Our data confirm that genes encoding orthologs to these also are enriched among the synaptic activity-regulated IE genes in humans. The induced transcription factors are in turn expected to regulate genes that produce the adaptive response. In mouse excitatory and inhibitory neurons the adaptive transcriptional responses are different (Spiegel et al., 2014), indicating that neuron type-specific activity-dependent gene regulation occurs. We found that the mouse orthologs of 15.7% of the hiPSCd neuron late-response genes have no evidence for neuronal activity-dependent regulation. It could be that, because the hiPSCd neurons are relatively immature, this cell type-specific part of the response is developmental stage specific rather than species specific. However, the genes upregulated only in hiPSCd neurons were over-represented by genes that have a neuron-enriched H3K4me3 promoter mark in the human brain throughout development as well as in the adult. First, this means that these genes presumably have neuronal functions. Second, this suggests that a considerable fraction of hiPSCd neuron-specifically synaptic activity-regulated genes are accessible for regulation during the course of the entire lifespan and are unlikely to be exclusively

responsive to activity during neuronal maturation. Besides, the genes that were upregulated only in hiPSCd neurons displayed enrichment for genes that are accompanied by human-specific epigenetic gains in the human brain (Reilly et al., 2015), suggesting that they might include genes whose regulation, possibly including activity-dependent regulation, is species specific.

Our data suggest that acquisition of lineage-specific synapse-to-nucleus signaling target genes and differences in synaptic activity-dependent regulation of common targets contribute to the phenotypic differences of humans compared to mice. We provide some outstanding examples supporting this view. First, one of the genes whose upregulation by synaptic activity was specific to hiPSCd neurons was *ADRA1B* (Table S7; Figure S7), which is associated with attention deficit/hyperactivity disorder (Mick et al., 2010). If *ADRA1B* is activity regulated in vivo, it could be involved in the regulation of mood, cognition, and behavior as an activity-induced component of the monoaminergic system in humans that is not synaptic activity dependent in mice (but see Kobori et al., 2011 and Shen and Gundlach, 1998). Second, we detected *CAMTA1*, which is associated with human episodic memory performance (Huentelman et al., 2007) and intellectual disability (Thevenon et al., 2012), to be upregulated by activity in hiPSCd neurons but not in mouse neurons (Table S7). This is exciting because *CAMTA1* is linked to a conserved noncoding sequence with accelerated evolution in humans (Prabhakar et al., 2006), has several putative enhancer regions with human-specific epigenetic gains (Reilly et al., 2015), and knockdown of *Camta1* in the mouse hippocampus specifically alters long-term memory (Bas-Orth et al., 2016), making *CAMTA1* a good candidate for a factor that adjusts episodic memory in a human-specific, synaptic activity-dependent manner. Third, *HIC1*, the gene with a prolonged increase in mRNA levels after synaptic activity in hiPSCd neurons compared to mouse neurons (Figure S7), negatively regulates expression of reelin receptor genes (Dubuissez et al., 2013). Since reelin is essential for the lamination of the cortex and has roles in neuronal maturation and synaptic functions (Förster et al., 2010), *HIC1* may be involved in brain cortex development. Moreover, Miller-Dieker syndrome (MDS) with lissencephaly as part of the phenotype is caused by haploinsufficiency of the genomic locus encompassing *HIC1* (Yingling et al., 2003). Although heterozygous loss of the *PAFAH1B1* (alias *LIS1*) and *YWHAE* (alias *14-3-3ε*) genes is believed to cause lissencaphaly in MDS, there is evidence that it also can result from a deletion not involving these but the *HIC1* gene (DECIPHER 250068; Firth et al., 2009). Collectively, these examples accentuate that some of the potentially human lineage-specifically regulated genes uncovered in this study take part in brain functions or developmental processes that could account for the superior cognitive abilities of humans compared to other mammals. Thus, the evolution of synaptic activity-regulated adaptogenomics may have driven the evolution of cognition.

In conclusion, this study demonstrates that the generic transcriptional response to evolutionarily conserved synapse-to-nucleus signaling has lineage-specific features in human neurons. This confirms that inherent genetic differences have an impact on synaptic activity-dependent transcription, providing a mechanism of how they may tune adaptive, plasticity-related brain functions.

EXPERIMENTAL PROCEDURES

Human iPSCs

The iPSC lines hiPS D1 and hiPS 3 were obtained from Dr. Jochen Utikal (DKFZ). hiPS D1 was generated from healthy human fibroblasts with an inducible polycistronic lentiviral reprogramming vector encoding for KLF4, MYC, POU5F1, and SOX2 (Horschitz et al., 2015). hiPS 3 was generated from healthy human melanocytes with inducible lentiviral reprogramming vectors encoding for KLF4, MYC, and POU5F1 (Utikal et al., 2009).

Generation of NPCs

We differentiated iPSCs to NPCs using a slightly modified spin embryoid body protocol (Kim et al., 2011) with dual SMAD inhibition (Chambers et al., 2009), as specified in the Supplemental Experimental Procedures.

Neuronal Differentiation

Differentiation of NPCs was initiated by plating 50,000 cells/cm^2 on poly-ornithine- (0.1 mg/mL) and laminin- (10 μg/mL) (both Sigma-Aldrich) coated (PO/Lam) dishes in NPC medium (see the Supplemental Experimental Procedures) without EGF and FGF2. After 1 week with medium changes every other day, cells were replated 75,000 cells/cm^2 on PO/Lam dishes or coverslips in neuronal differentiation (ND) medium (Neurobasal, Glutamax [1 mM], B27-vitamin A [2%], Pen/Strep [1:200; all Thermo Fisher Scientific], ascorbic acid [200 μM, Sigma-Aldrich], and BDNF [10 ng/mL, PeproTech]). Differentiation was allowed to proceed for up to 9 more weeks with medium changes three times per week. See also Figure S1.

Mixed-Species Culture

P0 mouse primary hippocampal cells, 75,000 cells/cm^2, were added to hiPSCd neurons in ND medium for the last 10 days of differentiation; 10 days in vitro is sufficient for inducing AP bursting in mouse primary neuron cultures with Bic/4AP (Arnold et al., 2005).

RNA-Seq Data Differential Gene Expression Analysis

RNA-seq was performed on four biological replicates of untreated and 1-hr Bic/4AP-treated mixed-species or hiPSCd neuron-only culture samples and three biological replicates of 4-hr Bic/4AP-treated mixed-species or hiPSCd neuron-only culture samples (GEO: GSE88773). TopHat2 (version 2.0.9) (Kim et al., 2013), HTSeq-count (HTSeq version 0.6.0 or 0.6.1) (Anders et al., 2015), and DESeq2 (version 1.8.1) (Love et al., 2014) were used for RNA-seq read mapping, counting, and differential gene expression analysis, respectively. The co-culture sample reads were filtered for either human or mouse reads as specified in the Supplemental Experimental Procedures.

Patch-Clamp Recordings

Whole-cell patch-clamp recordings were made at 32°C from cells plated on glass coverslips and secured with a platinum ring in a recording chamber (Open access chamber-1, Science Products) with heated in-line perfusion (32°C, TC324B, Warner Instruments) running constantly at 2 mL/min.

Statistical Analyses

Two samples were compared with two-tailed Student's or Welch's t test. If indicated, Holm-Sidak p adjustment was applied. Multiple samples were compared with one-way ANOVA and Dunnett's or Tukey's test, two-way ANOVA and Tukey's test, or two-way ANOVA on ranks and Holm-Sidak test. In RNA-seq data analysis, default statistical approaches of DESeq2 were applied.

Additional Details

Additional details about our methods are in the Supplemental Experimental Procedures.

ACCESSION NUMBERS

The accession number for the RNA sequencing data reported in this paper is GEO: GSE88773.

SUPPLEMENTAL INFORMATION

Supplemental Information includes Supplemental Experimental Procedures, seven figures, and seven tables and can be found with this article online at http://dx.doi.org/10.1016/j.celrep.2016.12.018.

AUTHOR CONTRIBUTIONS

H.B. conceived the study. P.P. and C.P.B. performed and analyzed the experiments. P.P., C.P.B., and H.B. designed the experiments, interpreted the data, and wrote the paper.

ACKNOWLEDGMENTS

We thank Dr. Utikal for hiPSCs, Dr. Galach and D. Roth for support in culturing hiPSCs, Dr. Horschitz for know-how on the generation of NPCs, I. Bünzli-Ehret for preparing primary neurons, V. Bantavi for technical assistance, Dr. Calogero for ideas on mixed-species RNA-seq analysis, and the nCounter Core Facility in Heidelberg. This work was supported by an ERC Advanced Grant (H.B.), a German-Israeli Project Cooperation (BA 1007/7-1), a fellowship by the Excellence Cluster CellNetworks at Heidelberg University (P.P.), and the SFB 1134. H.B. is a member of the Excellence Cluster *CellNetworks* at Heidelberg University.

Received: July 16, 2016
Revised: October 28, 2016
Accepted: December 6, 2016
Published: January 3, 2017

REFERENCES

Anders, S., Pyl, P.T., and Huber, W. (2015). HTSeq–a Python framework to work with high-throughput sequencing data. Bioinformatics *31*, 166–169.

Arnold, F.J., Hofmann, F., Bengtson, C.P., Wittmann, M., Vanhoutte, P., and Bading, H. (2005). Microelectrode array recordings of cultured hippocampal networks reveal a simple model for transcription and protein synthesis-dependent plasticity. J. Physiol. *564*, 3–19.

Bading, H. (2013). Nuclear calcium signalling in the regulation of brain function. Nat. Rev. Neurosci. *14*, 593–608.

Bading, H., Ginty, D.D., and Greenberg, M.E. (1993). Regulation of gene expression in hippocampal neurons by distinct calcium signaling pathways. Science *260*, 181–186.

Bae, B.I., Jayaraman, D., and Walsh, C.A. (2015). Genetic changes shaping the human brain. Dev. Cell *32*, 423–434.

Balik, A., Penn, A.C., Nemoda, Z., and Greger, I.H. (2013). Activity-regulated RNA editing in select neuronal subfields in hippocampus. Nucleic Acids Res. *41*, 1124–1134.

Bas-Orth, C., Tan, Y.W., Oliveira, A.M., Bengtson, C.P., and Bading, H. (2016). The calmodulin-binding transcription activator CAMTA1 is required for long-term memory formation in mice. Learn. Mem. *23*, 313–321.

Ben-Ari, Y., Gaiarsa, J.L., Tyzio, R., and Khazipov, R. (2007). GABA: a pioneer transmitter that excites immature neurons and generates primitive oscillations. Physiol. Rev. *87*, 1215–1284.

Chambers, S.M., Fasano, C.A., Papapetrou, E.P., Tomishima, M., Sadelain, M., and Studer, L. (2009). Highly efficient neural conversion of human ES and iPS cells by dual inhibition of SMAD signaling. Nat. Biotechnol. *27*, 275–280.

Cheung, I., Shulha, H.P., Jiang, Y., Matevossian, A., Wang, J., Weng, Z., and Akbarian, S. (2010). Developmental regulation and individual differences of neuronal H3K4me3 epigenomes in the prefrontal cortex. Proc. Natl. Acad. Sci. USA *107*, 8824–8829.

De Cesare, D., and Sassone-Corsi, P. (2000). Transcriptional regulation by cyclic AMP-responsive factors. Prog. Nucleic Acid Res. Mol. Biol. *64*, 343–369.

Dubuissez, M., Faiderbe, P., Pinte, S., Dehennaut, V., Rood, B.R., and Leprince, D. (2013). The Reelin receptors ApoER2 and VLDLR are direct target genes of HIC1 (Hypermethylated In Cancer 1). Biochem. Biophys. Res. Commun. *440*, 424–430.

Firth, H.V., Richards, S.M., Bevan, A.P., Clayton, S., Corpas, M., Rajan, D., Van Vooren, S., Moreau, Y., Pettett, R.M., and Carter, N.P. (2009). DECIPHER: database of chromosomal imbalance and phenotype in humans using Ensembl resources. Am. J. Hum. Genet. *84*, 524–533.

Förster, E., Bock, H.H., Herz, J., Chai, X., Frotscher, M., and Zhao, S. (2010). Emerging topics in Reelin function. Eur. J. Neurosci. *31*, 1511–1518.

Frank, D.A., and Greenberg, M.E. (1994). CREB: a mediator of long-term memory from mollusks to mammals. Cell *79*, 5–8.

Geschwind, D.H., and Rakic, P. (2013). Cortical evolution: judge the brain by its cover. Neuron *80*, 633–647.

Hardingham, G.E., Arnold, F.J., and Bading, H. (2001). Nuclear calcium signaling controls CREB-mediated gene expression triggered by synaptic activity. Nat. Neurosci. *4*, 261–267.

Hardingham, G.E., Fukunaga, Y., and Bading, H. (2002). Extrasynaptic NMDARs oppose synaptic NMDARs by triggering CREB shut-off and cell death pathways. Nat. Neurosci. *5*, 405–414.

Horschitz, S., Matthäus, F., Groß, A., Rosner, J., Galach, M., Greffrath, W., Treede, R.D., Utikal, J., Schloss, P., and Meyer-Lindenberg, A. (2015). Impact of preconditioning with retinoic acid during early development on morphological and functional characteristics of human induced pluripotent stem cell-derived neurons. Stem Cell Res. (Amst.) *15*, 30–41.

Huentelman, M.J., Papassotiropoulos, A., Craig, D.W., Hoerndli, F.J., Pearson, J.V., Huynh, K.D., Corneveaux, J., Hänggi, J., Mondadori, C.R., Buchmann, A., et al. (2007). Calmodulin-binding transcription activator 1 (CAMTA1) alleles predispose human episodic memory performance. Hum. Mol. Genet. *16*, 1469–1477.

Kim, T.K., Hemberg, M., Gray, J.M., Costa, A.M., Bear, D.M., Wu, J., Harmin, D.A., Laptewicz, M., Barbara-Haley, K., Kuersten, S., et al. (2010). Widespread transcription at neuronal activity-regulated enhancers. Nature *465*, 182–187.

Kim, J.E., O'Sullivan, M.L., Sanchez, C.A., Hwang, M., Israel, M.A., Brennand, K., Deerinck, T.J., Goldstein, L.S., Gage, F.H., Ellisman, M.H., and Ghosh, A. (2011). Investigating synapse formation and function using human pluripotent stem cell-derived neurons. Proc. Natl. Acad. Sci. USA *108*, 3005–3010.

Kim, D., Pertea, G., Trapnell, C., Pimentel, H., Kelley, R., and Salzberg, S.L. (2013). TopHat2: accurate alignment of transcriptomes in the presence of insertions, deletions and gene fusions. Genome Biol. *14*, R36.

Kobori, N., Hu, B., and Dash, P.K. (2011). Altered adrenergic receptor signaling following traumatic brain injury contributes to working memory dysfunction. Neuroscience *172*, 293–302.

Lanahan, A., and Worley, P. (1998). Immediate-early genes and synaptic function. Neurobiol. Learn. Mem. *70*, 37–43.

Liu, X., Somel, M., Tang, L., Yan, Z., Jiang, X., Guo, S., Yuan, Y., He, L., Oleksiak, A., Zhang, Y., et al. (2012). Extension of cortical synaptic development distinguishes humans from chimpanzees and macaques. Genome Res. *22*, 611–622.

Love, M.I., Huber, W., and Anders, S. (2014). Moderated estimation of fold change and dispersion for RNA-seq data with DESeq2. Genome Biol. *15*, 550.

Maze, I., Wenderski, W., Noh, K.M., Bagot, R.C., Tzavaras, N., Purushothaman, I., Elsässer, S.J., Guo, Y., Ionete, C., Hurd, Y.L., et al. (2015). Critical role of histone turnover in neuronal transcription and plasticity. Neuron *87*, 77–94.

Mick, E., Todorov, A., Smalley, S., Hu, X., Loo, S., Todd, R.D., Biederman, J., Byrne, D., Dechairo, B., Guiney, A., et al. (2010). Family-based genome-wide association scan of attention-deficit/hyperactivity disorder. J. Am. Acad. Child Adolesc. Psychiatry *49*, 898–905.

Mo, J., Kim, C.H., Lee, D., Sun, W., Lee, H.W., and Kim, H. (2015). Early growth response 1 (Egr-1) directly regulates GABAA receptor α2, α4, and θ subunits in the hippocampus. J. Neurochem. *133*, 489–500.

Necsulea, A., and Kaessmann, H. (2014). Evolutionary dynamics of coding and non-coding transcriptomes. Nat. Rev. Genet. *15*, 734–748.

Prabhakar, S., Noonan, J.P., Pääbo, S., and Rubin, E.M. (2006). Accelerated evolution of conserved noncoding sequences in humans. Science *314*, 786.

Pruunsild, P., Sepp, M., Orav, E., Koppel, I., and Timmusk, T. (2011). Identification of cis-elements and transcription factors regulating neuronal activity-dependent transcription of human BDNF gene. J. Neurosci. *31*, 3295–3308.

Qiu, J., McQueen, J., Bilican, B., Dando, O., Magnani, D., Punovuori, K., Selvaraj, B.T., Livesey, M., Haghi, G., Heron, S., et al. (2016). Evidence for evolutionary divergence of activity-dependent gene expression in developing neurons. eLife *5*, e20337.

Reilly, S.K., Yin, J., Ayoub, A.E., Emera, D., Leng, J., Cotney, J., Sarro, R., Rakic, P., and Noonan, J.P. (2015). Evolutionary genomics. Evolutionary changes in promoter and enhancer activity during human corticogenesis. Science *347*, 1155–1159.

Reitmair, A., Sachs, G., Im, W.B., and Wheeler, L. (2012). C6orf176: a novel possible regulator of cAMP-mediated gene expression. Physiol. Genomics *44*, 152–161.

Rossner, M.J., Dörr, J., Gass, P., Schwab, M.H., and Nave, K.A. (1997). SHARPs: mammalian enhancer-of-split- and hairy-related proteins coupled to neuronal stimulation. Mol. Cell. Neurosci. *9*, 460–475.

Saha, R.N., Wissink, E.M., Bailey, E.R., Zhao, M., Fargo, D.C., Hwang, J.Y., Daigle, K.R., Fenn, J.D., Adelman, K., and Dudek, S.M. (2011). Rapid activity-induced transcription of Arc and other IEGs relies on poised RNA polymerase II. Nat. Neurosci. *14*, 848–856.

Shen, P.J., and Gundlach, A.L. (1998). Differential spatiotemporal alterations in adrenoceptor mRNAs and binding sites in cerebral cortex following spreading depression: selective and prolonged up-regulation of alpha1B-adrenoceptors. Exp. Neurol. *154*, 612–627.

Silbereis, J.C., Pochareddy, S., Zhu, Y., Li, M., and Sestan, N. (2016). The cellular and molecular landscapes of the developing human central nervous system. Neuron *89*, 248–268.

Spiegel, I., Mardinly, A.R., Gabel, H.W., Bazinet, J.E., Couch, C.H., Tzeng, C.P., Harmin, D.A., and Greenberg, M.E. (2014). Npas4 regulates excitatory-inhibitory balance within neural circuits through cell-type-specific gene programs. Cell *157*, 1216–1229.

Thevenon, J., Lopez, E., Keren, B., Heron, D., Mignot, C., Altuzarra, C., Béri-Dexheimer, M., Bonnet, C., Magnin, E., Burglen, L., et al. (2012). Intragenic CAMTA1 rearrangements cause non-progressive congenital ataxia with or without intellectual disability. J. Med. Genet. *49*, 400–408.

Utikal, J., Maherali, N., Kulalert, W., and Hochedlinger, K. (2009). Sox2 is dispensable for the reprogramming of melanocytes and melanoma cells into induced pluripotent stem cells. J. Cell Sci. *122*, 3502–3510.

Wang, J., Campos, B., Jamieson, G.A., Jr., Kaetzel, M.A., and Dedman, J.R. (1995). Functional elimination of calmodulin within the nucleus by targeted expression of an inhibitor peptide. J. Biol. Chem. *270*, 30245–30248.

West, A.E., and Greenberg, M.E. (2011). Neuronal activity-regulated gene transcription in synapse development and cognitive function. Cold Spring Harb. Perspect. Biol. *3*, a005744.

Wilson, M.D., and Odom, D.T. (2009). Evolution of transcriptional control in mammals. Curr. Opin. Genet. Dev. *19*, 579–585.

Yingling, J., Toyo-Oka, K., and Wynshaw-Boris, A. (2003). Miller-Dieker syndrome: analysis of a human contiguous gene syndrome in the mouse. Am. J. Hum. Genet. *73*, 475–488.

Zanzouri, M., Lauritzen, I., Duprat, F., Mazzuca, M., Lesage, F., Lazdunski, M., and Patel, A. (2006). Membrane potential-regulated transcription of the resting K+ conductance TASK-3 via the calcineurin pathway. J. Biol. Chem. *281*, 28910–28918.

Zhang, S.J., Steijaert, M.N., Lau, D., Schütz, G., Delucinge-Vivier, C., Descombes, P., and Bading, H. (2007). Decoding NMDA receptor signaling: identification of genomic programs specifying neuronal survival and death. Neuron *53*, 549–562.

Zhang, S.J., Zou, M., Lu, L., Lau, D., Ditzel, D.A., Delucinge-Vivier, C., Aso, Y., Descombes, P., and Bading, H. (2009). Nuclear calcium signaling controls expression of a large gene pool: identification of a gene program for acquired neuroprotection induced by synaptic activity. PLoS Genet. *5*, e1000604.

Cell Reports, Volume *18*

Supplemental Information

Networks of Cultured iPSC-Derived Neurons Reveal the Human Synaptic Activity-Regulated Adaptive Gene Program

Priit Pruunsild, C. Peter Bengtson, and Hilmar Bading

Figure S1

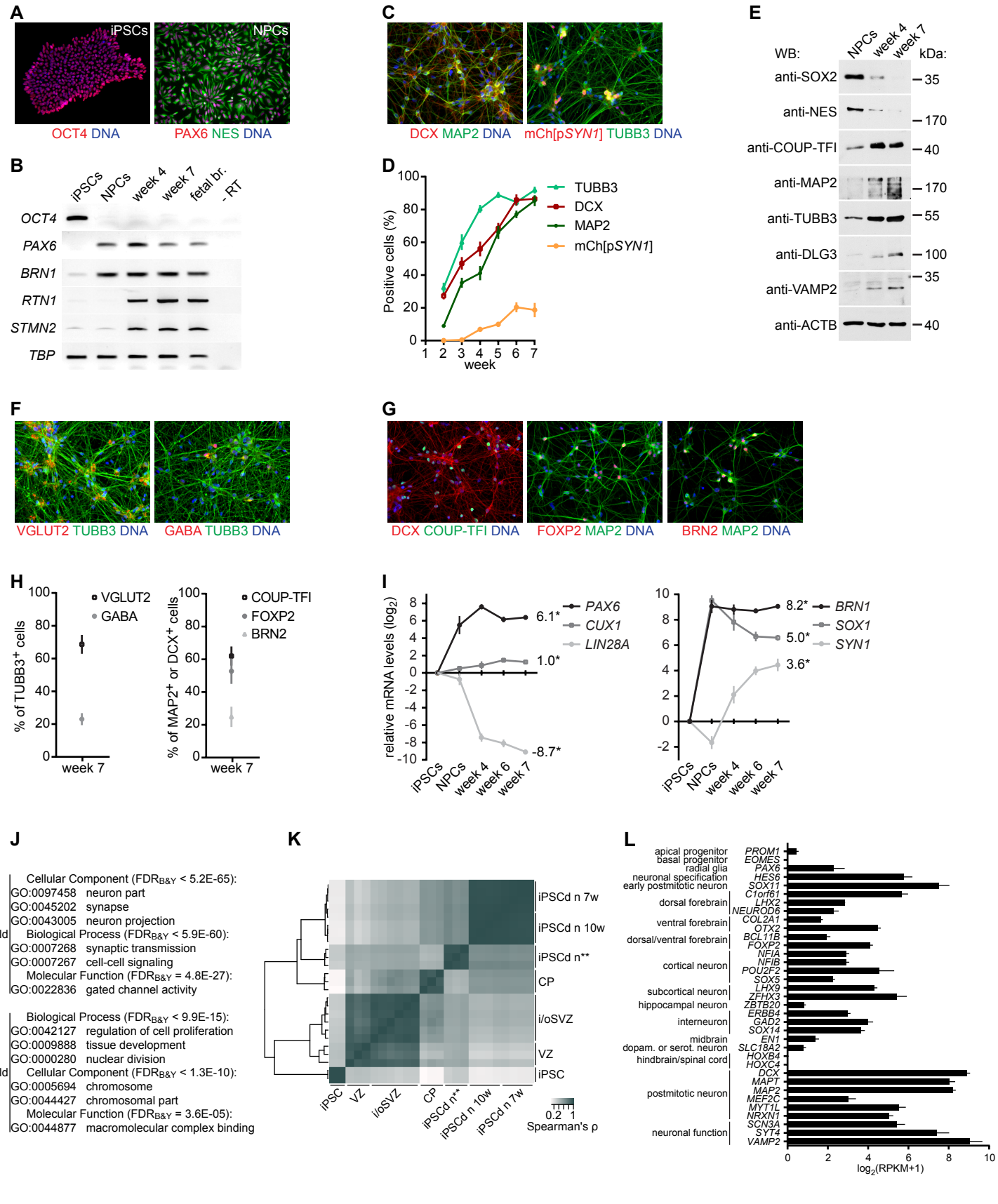
A
iPSCs
NPCs
OCT4 DNA
PAX6 NES DNA
C
DCX MAP2 DNA
mCh[pSYN1] TUBB3 DNA
E
WB:
NPCs
week 4
week 7
kDa:
anti-SOX2
35
anti-NES
170
anti-COUP-TFI
40
anti-MAP2
170
anti-TUBB3
55
anti-DLG3
100
anti-VAMP2
35
anti-ACTB
40
B
iPSCs
NPCs
week 4
week 7
fetal br.
-RT
OCT4
PAX6
BRN1
RTN1
STMN2
TBP
D
Positive cells (%)
week
TUBB3
DCX
MAP2
mCh[pSYN1]
F
VGLUT2 TUBB3 DNA
GABA TUBB3 DNA
G
DCX COUP-TFI DNA
FOXP2 MAP2 DNA
BRN2 MAP2 DNA
H
% of TUBB3+ cells
% of MAP2+ or DCX+ cells
week 7
VGLUT2
GABA
COUP-TFI
FOXP2
BRN2
I
relative mRNA levels (log2)
PAX6
CUX1
LIN28A
6.1*
1.0*
-8.7*
BRN1
SOX1
SYN1
8.2*
5.0*
3.6*
iPSCs
NPCs
week 4
week 6
week 7
J
Cellular Component (FDRB&Y < 5.2E-65):
GO:0097458 neuron part
GO:0045202 synapse
GO:0043005 neuron projection
>8-fold
Biological Process (FDRB&Y < 5.9E-60):
GO:0007268 synaptic transmission
GO:0007267 cell-cell signaling
Molecular Function (FDRB&Y = 4.8E-27):
GO:0022836 gated channel activity
Biological Process (FDRB&Y < 9.9E-15):
GO:0042127 regulation of cell proliferation
GO:0009888 tissue development
GO:0000280 nuclear division
>8-fold
Cellular Component (FDRB&Y < 1.3E-10):
GO:0005694 chromosome
GO:0044427 chromosomal part
Molecular Function (FDRB&Y = 3.6E-05):
GO:0044877 macromolecular complex binding
K
iPSCd n 7w
iPSCd n 10w
iPSCd n**
CP
i/oSVZ
VZ
iPSC
iPSC
VZ
i/oSVZ
CP
iPSCd n**
iPSCd n 10w
iPSCd n 7w
Spearman's ρ
0.2
1
L
apical progenitor
basal progenitor
radial glia
neuronal specification
early postmitotic neuron
dorsal forebrain
ventral forebrain
dorsal/ventral forebrain
cortical neuron
subcortical neuron
hippocampal neuron
interneuron
midbrain
dopam. or serot. neuron
hindbrain/spinal cord
postmitotic neuron
neuronal function
PROM1
EOMES
PAX6
HES6
SOX11
C1orf61
LHX2
NEUROD6
COL2A1
OTX2
BCL11B
FOXP2
NFIA
NFIB
POU2F2
SOX5
LHX9
ZFHX3
ZBTB20
ERBB4
GAD2
SOX14
EN1
SLC18A2
HOXB4
HOXC4
DCX
MAP1
MAP2
MEF2C
MYT1L
NRXN1
SCN3A
SYT4
VAMP2
log2(RPKM+1)

Figure S1. Molecular characterization of hiPSCd neuron differentiation. Related to Experimental Procedures
(A) Immunofluorescence staining of iPSCs and neuronal precursor cells (NPCs) with antibodies recognizing the indicated proteins. Human iPSCs (hiPS D1, see Experimental Procedures) were differentiatiated into PAX6- and nestin (NES)-expressing NPCs using a spin embryoid body protocol (Kim et al., 2011) with dual SMAD inhibition (Chambers et al., 2009).
(B) RT-PCR analysis of mRNA levels in iPSCs, NPCs and NPCs differentiated for 4 and 7 weeks, or in human fetal brain with primers targeting the indicated genes. A reaction without reverse transcription (-RT) was used as a control.
(C) Immunofluorescence staining of hiPSCd neurons differentiated for 7 weeks from NPCs with antibodies recognizing the indicated proteins. Expression of DCX and MAP2, or mCherry (direct fluorescence) under the control of the human *SYN1* promoter (mCh[p*SYN1*], lentiviral infection of NPCs) and TUBB3 is shown. Of note, expression of EGFP was very similar to expression of mCherry when NPCs were infected with a lentivirus encoding for EGFP under the control of p*SYN1*. See also Figure 3G.
(D) Quantification of cells positive for the indicated proteins in cultures of hiPSCd neurons differentiated for 2 to 7 weeks from NPCs. Three or four biological replicates were used for the quantification at each time point (mean ± SEM).
(E) Western blot analysis of protein expression using lysates from NPCs and hiPSCd neurons differentiated for 4 or 7 weeks from NPCs with antibodies recognizing the indicated proteins.
(F and G) Immunofluorescence staining of hiPSCd neurons differentiated for 7 weeks from NPCs with antibodies recognizing the indicated antigens.
(H) Quantification of cells double-positive for TUBB3, MAP2 or DCX and the indicated antigen in cultures of hiPSCd neurons differentiated for 7 weeks from NPCs. TUBB3 and VGLUT2, TUBB3 and GABA, DCX and COUP-TFI, MAP2 and FOXP2, or MAP2 and BRN2 were assessed. Three biological replicates were used for the quantification at each time point (mean ± SEM).
(I) RT-qPCR analysis of mRNA levels in hiPSCs, NPCs and hiPSCd neurons differentiated for 4, 6 or 7 weeks from NPCs with primers targeting the indicated genes. mRNA levels relative to the levels measured from iPSCs are shown for each gene. The values marked with asterisks designate the $\log_2$ fold changes measured with RNA-Seq in the respective genes' mRNA levels in hiPSCd neurons differentiated for 7 weeks from NPCs relative to the levels measured from iPSCs. Two or three biological replicates were used at each time point (mean ± SEM).
(J) GO term over-representation analysis with ToppGene (Chen et al., 2009) among genes up- or downregulated more than 8-fold in hiPSCd neurons differentiated for 7 weeks from NPCs relative to the expression levels in iPSCs. Most significantly enriched GO terms are shown. See also Table S1.
(K) Spearman correlation between the transcriptomes of the iPSCs (n = 2) and hiPSCd neurons (iPSCd n) produced in this study (7w and 10w, 7th and 10th week of differentiation from NPCs, respectively, both n = 4), hiPSCd neuron samples from Wen et al., 2014 (iPSCn**, four weeks of differentiation, n = 3), and human fetal (13th to 16th week postconception) ventricular zone (VZ, n = 3), inner or outer subventricular zone (i/o SVZ, n = 6) or cortical plate (CP, n = 3) samples from Fietz et al., 2012. 4497 genes with log-transformed RNA-Seq read counts per million standard deviation > 1 were used for the analysis. Correlation between all our hiPSCd neuron samples, ρ 0.968 to 0.998. Our hiPSCd neurons *vs* hiPSCd neurons produced by Wen et al. (ρ up to 0.712). Our hiPSCd neurons *vs* human 13th to 16th week postconception fetus cortical plate, which contains mostly postmitotic neurons (ρ up to 0.646). Our hiPSCd neurons *vs* human 13th to 16th week postconception fetus ventricular and subventricular zones, which contain proliferating cells (ρ up to 0.509).
(L) mRNA levels of selected marker genes in hiPSCd neurons differentiated for 7 weeks according to RNA-Seq (n = 4, mean ± SEM). Marker genes were selected based on single-cell transcriptomes of *in vivo* and *in vitro* human neurons (Camp et al., 2016), and additionally, some classical brain region-specific markers, used for example to identify regional specificity of human PSC-derived neurons (Imaizumi et al., 2015), were included. This data indicates that the hiPSCd neuron cultures are a heterogeneous population of neurons representing dorsal as well as ventral developing forebrain.

A brief description of markers whose expression was assessed in panels other than L: *OCT4* (*POU5F1*) and *LIN28A*, pluripotency markers; *PAX6* and *BRN1* (*POU3F3*), neuron/brain development-associated genes; *RTN1* and *STMN2*, neuron-specifically expressed genes; DCX and MAP2, postmitotic neuron markers; TUBB3, neuronal lineage-expressed protein; SOX2 and NES, NPC-expressed proteins; COUP-TFI (NR2F1), developing forebrain-enriched protein; DLG3, VAMP2 and SYN1, synaptic proteins; VGLUT2 (SLC17A6), excitatory neuron marker; GABA, inhibitory neuron marker; FOXP2 and BRN2 (POU3F2), forebrain-enriched/cortical layer markers; *SOX1*, NPC marker; *CUX1*, cell differentiation regulator.

Figure S2

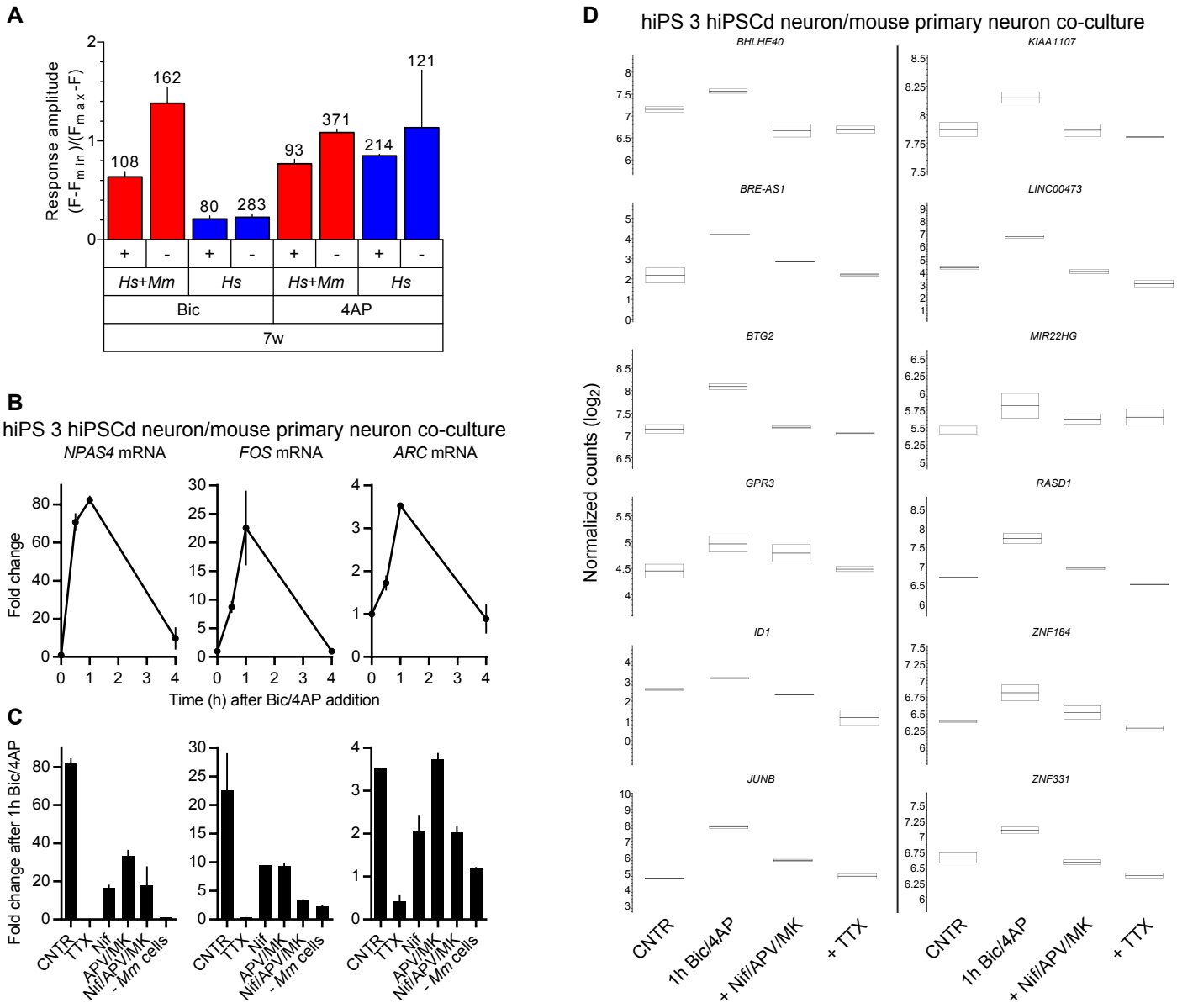

Figure S2.

(A) Rhod2 Ca^{2+} imaging of responses to bicuculline (Bic, 50 µM) or 4-aminopyridine (4AP, 250 µM).

Related to Figure 2

Ca^{2+} response amplitudes (peak minus baseline, mean ± SEM) in the number of cells indicated for $EGFP^{+}$ (+) and $EGFP^{-}$ (-) cells in the 7w *Hs*+*Mm* or *Hs* cultures and in the 10w *Hs* cultures. 7w and 10w, NPCs were differentiated for 7 weeks and 10 weeks, respectively. *Hs*+*Mm*, co-culture of hiPSCd neurons with mouse primary hippocampal neurons; *Hs*, human iPSCd neuron-only culture.

(B - D) Excitatory synaptic input to hiPS 3-derived hiPSCd neurons upregulates human IE genes.

Related to Figures 3 and 4

RT-qPCR (B and C) and nCounter (D, Kulkarni et al., 2011) analyses of changes in human IE gene mRNA levels after treatment with Bic/4AP (bicuculline, 50 µM and 4-aminopyridine, 250 µM) of hiPS 3-derived 7 week hiPSCd neuron/mouse primary hippocampal neuron co-cultures.

(B) Temporal profiles of IE gene mRNA levels in response to enhancement of synaptic activity.

(C and D) Analysis of the effects of blocking action potentials (TTX, tetrodotoxin, 1 µM), VGCCs (C, Nif, Nifedipine, 10 µM) or NMDARs (C, APV/MK, 2-amino-5-phosphonovalerate, 50 µM and MK801, 10 µM), or both VGCCs and NMDARs (Nif/APV/MK) on the increase in IE gene mRNA levels in response to Bic/4AP-tretament. In C, IE gene mRNA level changes in hiPS 3-derived hiPSCd neurons differentiated for 7 weeks and maintained without addition of mouse primary hippocampal neurons (- *Mm* cells) are also shown. In D, + shows that the indicated substances were present in the culture medium in addition to Bic/4AP.

Two biological replicate measurements were performed for all data points (B and C, mean ± SEM; C, data range with average).

Figure S3

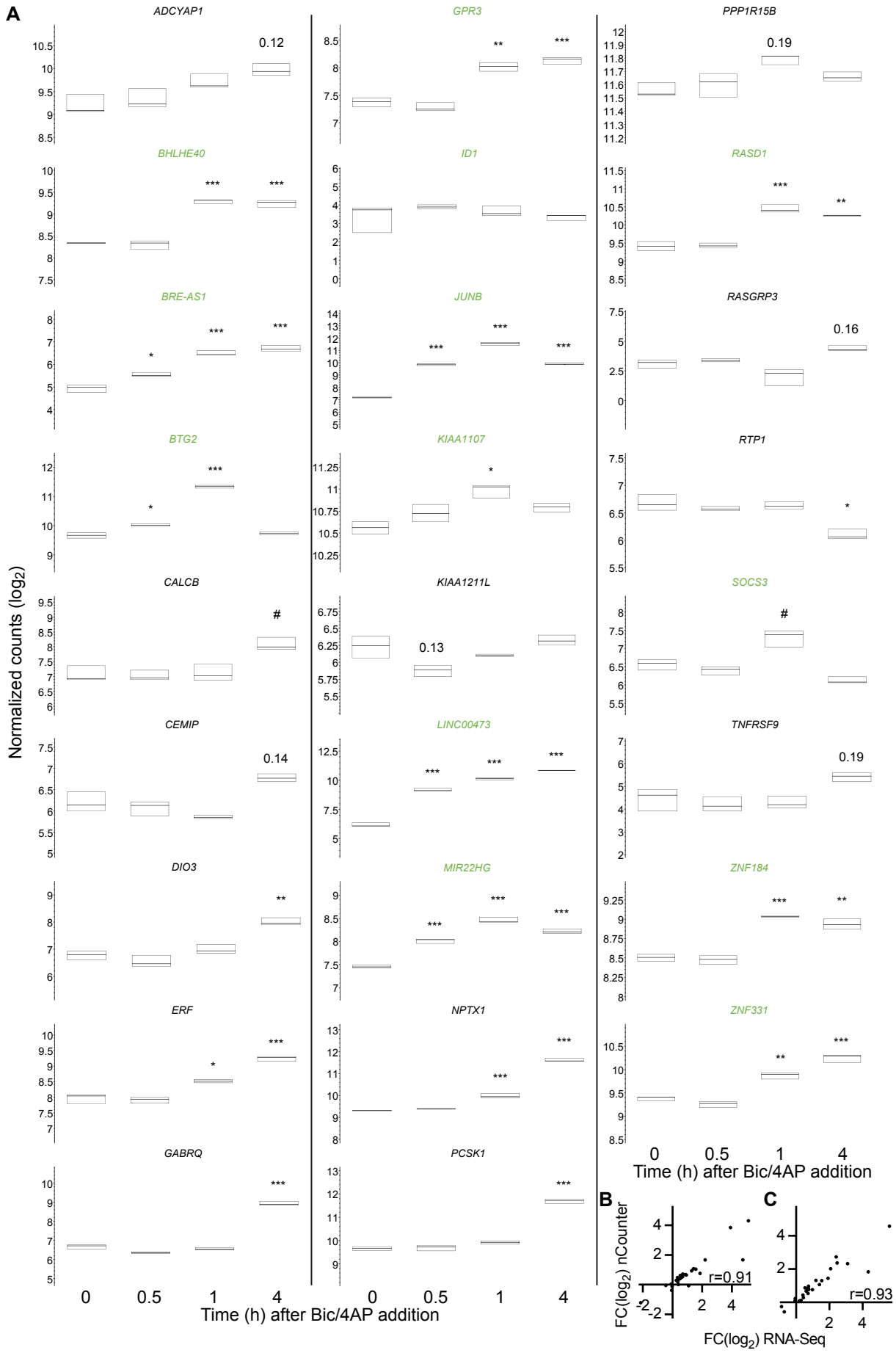
A
ADCYAP1
GPR3
PPP1R15B
BHLHE40
ID1
RASD1
BRE-AS1
JUNB
RASGRP3
BTG2
KIAA1107
RTP1
CALCB
KIAA1211L
SOCS3
CEMIP
LINC00473
TNFRSF9
DIO3
MIR22HG
ZNF184
ERF
NPTX1
ZNF331
GABRQ
PCSK1
Normalized counts (log2)
Time (h) after Bic/4AP addition
B
C
FC(log2) nCounter
FC(log2) RNA-Seq
r=0.91
r=0.93

Figure S3. Analysis of RNA levels of the indicated human genes with the nCounter method (Kulkarni et al., 2011). Related to Figure 4

(A) 7 week hiPSCd neuron/mouse primary hippocampal neuron co-culture was left untreated or treated with Bic/4AP (bicuculline, 50 μM and 4-aminopyridine, 250 μM) for the time indicated. RNA expression levels were normalized to the levels of three "housekeeping" genes: *EIF2B4*, *FCF1*and *HPRT1* (normalized counts). The names of human IE genes according to RNA-Seq data are in green. Three biological replicate measurements were performed for each data point. Box plots show data range with median. Significance (one-way ANOVA and Dunnett's multiple comparison test) is indicated compared to untreated control, #$p < 0.1$, *$p < 0.05$, **$p < 0.01$, ***$p < 0.001$. Values above boxes are p values (shown if < 0.2 and > 0.1).

(B and C) Correlation of gene expression fold change $\log_2$ [FC($\log_2$)] values of 26 human genes measured using the nCounter method after a one-hour Bic/4AP-treatment (B) or after a four-hour Bic/4AP-treatment (C) with the corresponding values measured with RNA-Seq. The dots denote the mean values of three biological replicate experiments. Pearson's r two-tailed $p < 0.0001$. The mean fold changes in gene expression obtained with the two methods at both the one hour and the four hours time point are very similar, verifying the reliability of the mixed-species RNA-Seq analysis.

Figure S4

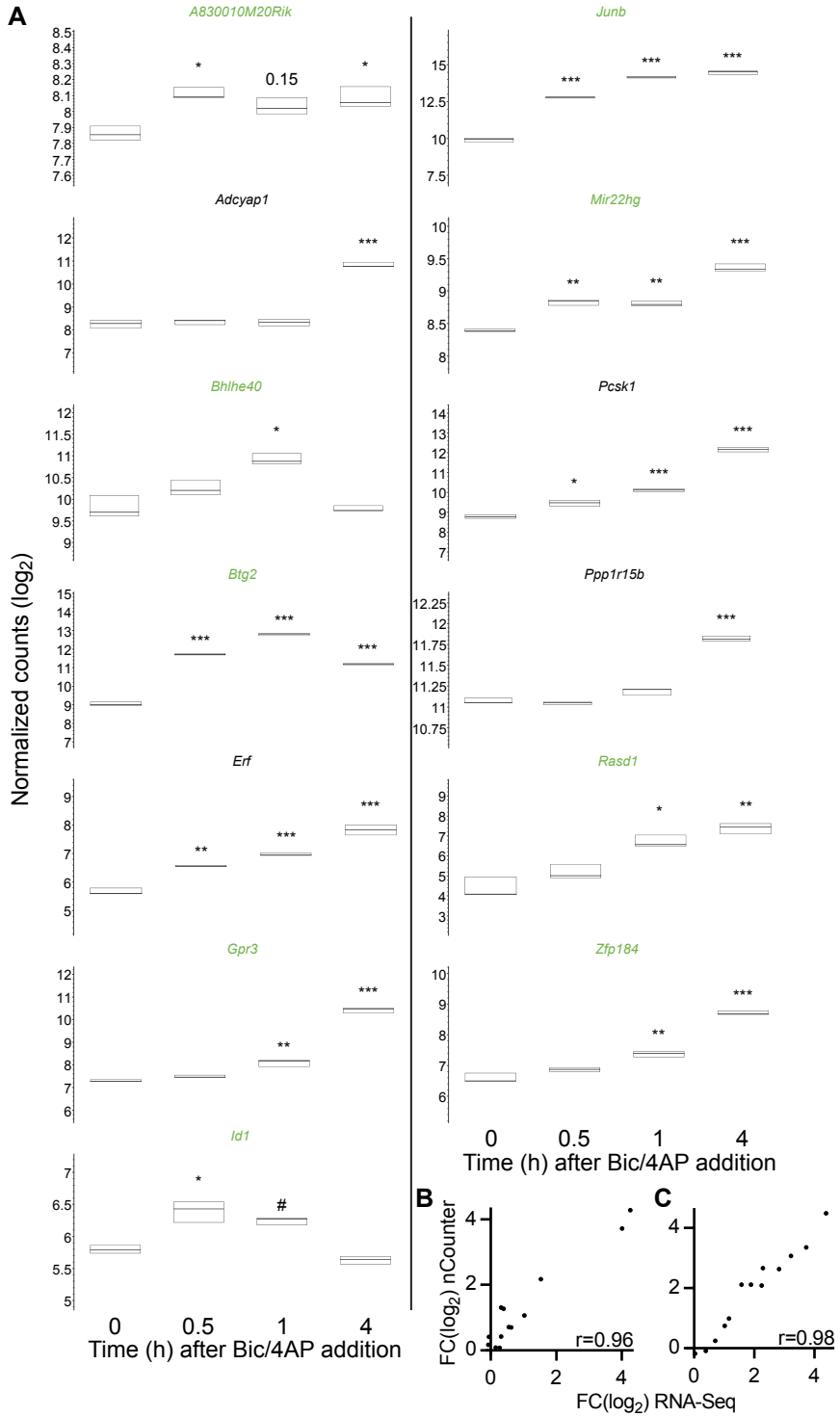

Figure S4. Analysis of RNA levels of the indicated mouse genes with the nCounter method (Kulkarni et al., 2011). Related to Figure 4

(A) 7 week hiPSCd neuron/mouse primary hippocampal neuron co-culture was left untreated or treated with Bic/4AP (bicuculline, 50 µM and 4-aminopyridine, 250 µM) for the time indicated. RNA expression levels were normalized to the levels of three "housekeeping" genes: *Eif2b4*, *Fcf1* and *Hprt1* (normalized counts). The names of the mouse orthologs of human IE genes are in green. Three biological replicate measurements were performed for each data point. Box plots show data range with median. Significance (one-way ANOVA and Dunnett's multiple comparison test) is indicated compared to untreated control, #$p < 0.1$, *$p < 0.05$, **$p < 0.01$, ***$p < 0.001$. 0.15, p value for the respective data point. All 9 mouse orthologs of human IE genes analysed, including genes that were not significantly induced at the one hour time point in RNA-Seq analysis, showed significantly upregulated RNA levels at 30 minutes and/or one hour after Bic/4AP addition.

(B and C) Correlation of gene expression fold change $\log_2$ [FC($\log_2$)] values of 13 mouse genes measured using the nCounter method after a one-hour Bic/4AP-treatment (B) or after a four-hour Bic/4AP-treatment (C) with the corresponding values measured with RNA-Seq. The dots denote the mean values of three biological replicate experiments. Pearson's r two-tailed $p < 0.0001$. The mean fold changes in gene expression obtained with the two methods at both the one hour and the four hours time point are very similar, verifying the reliability of the mixed-species RNA-Seq analysis.

Figure S5

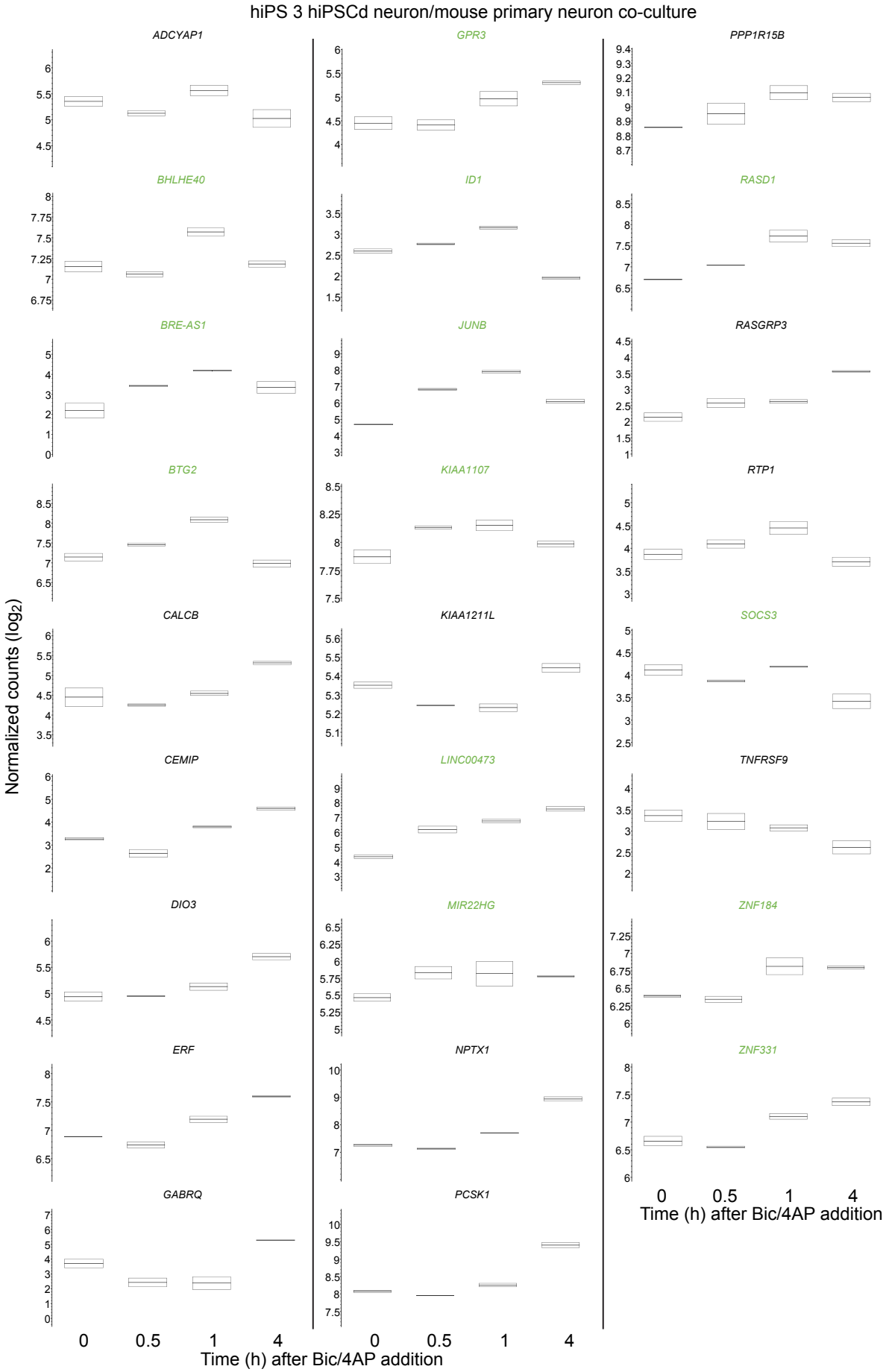
hiPS 3 hiPSCd neuron/mouse primary neuron co-culture
ADCYAP1
GPR3
PPP1R15B
BHLHE40
ID1
RASD1
BRE-AS1
JUNB
RASGRP3
BTG2
KIAA1107
RTP1
CALCB
KIAA1211L
SOCS3
CEMIP
LINC00473
TNFRSF9
DIO3
MIR22HG
ZNF184
ERF
NPTX1
ZNF331
GABRQ
PCSK1
Normalized counts (log2)
0
0.5
1
4
Time (h) after Bic/4AP addition

Figure S5. Analysis of RNA levels of the indicated human genes with the nCounter method (Kulkarni et al., 2011) in hiPS 3-derived 7 week hiPSCd neuron/mouse primary hippocampal neuron co-culture. Related to Figure 4
The cells were left untreated or treated with Bic/4AP (bicuculline, 50 μM and 4-aminopyridine, 250 μM) for the time indicated. RNA expression levels were normalized to the levels of three "housekeeping" genes: *EIF2B4*, *FCF1* and *HPRT1* (normalized counts). The names of the human IE genes according to RNA-Seq data obtained with the hiPS D1-derived hiPSCd neurons are in green. Two biological replicate measurements were performed for each data point. Box plots show data range with average.

Figure S6

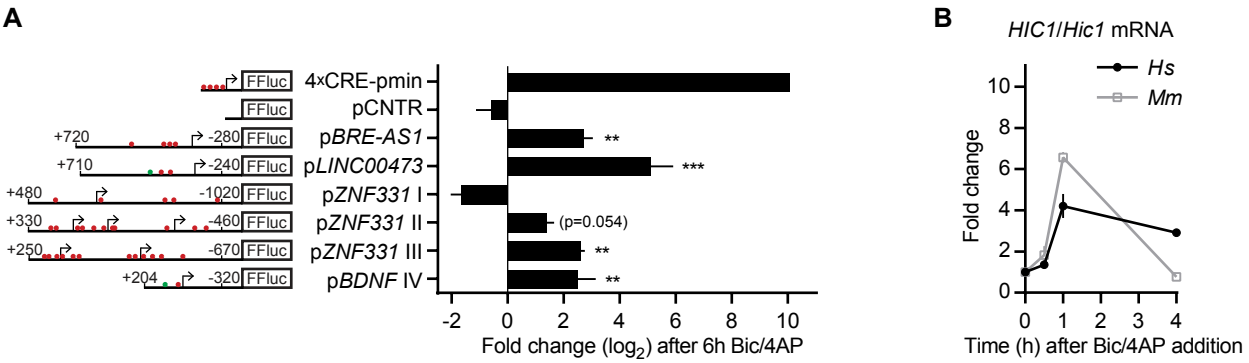

Figure S6. Assessment of potential lineage-specific control of synaptic activity-regulated genes.
Related to Figures 5 and 7

(A) Luciferase reporter assay with the firefly luciferase (FFluc) under the control of the indicated promoter or without a promoter (pCNTR) in mouse primary cortical neurons. Change in FFluc activity in response to Bic/4AP-treatment (bicuculline, 50 µM and 4-aminopyridine, 250 µM) is shown. Arrows denote transcription start sites (TSSs). Numbers specify bps upstream (-) or downstream (+) of the most 5' or 3' TSS, respectively. Red or green dots represent CRE and CREhs or PasRE cis-elements, respectively. n = 3; mean ± SEM; one-way ANOVA and Dunnett's multiple comparison test, **$p < 0.01$, ***$p < 0.001$. The asterisks indicate significance compared to pCNTR.

(B) RT-qPCR analysis of *HIC1*/*Hic1* mRNA levels in hiPS 3-derived hiPSCd neuron/mouse primary hippocampal neuron co-culture. Changes in human (*Hs*) *HIC1* and mouse (*Mm*) *Hic1* mRNA levels after treatment with Bic/4AP (bicuculline, 50 µM and 4-aminopyridine, 250 µM) for the time indicated are shown. n = 2, mean ± SEM.

Figure S7

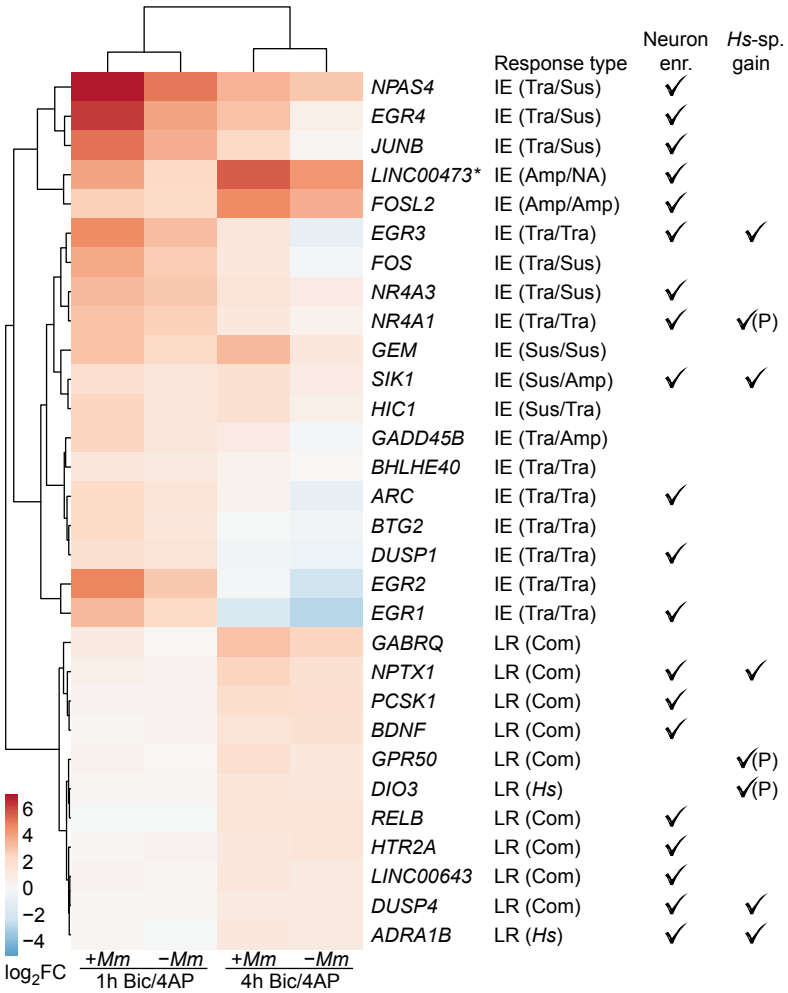

Figure S7. Core set of human iPSC-derived neuron synaptic activity-regulated genes.
Related to Figures 4 and 6, and to Discussion
Heat map of the expression level changes of 30 human genes with the most consistent responses [> two-fold expression change with $p_{adj} < 0.01$ both in the mixed-species culture (+*Mm*) and in the hiPSCd neuron-only culture (-*Mm*)] to synaptic activity in hiPSCd neurons after one hour and/or four hours of Bic/4AP-treatment. The temporal profiles of the expression level changes (Response type) in the mixed-species culture is specified for both the human gene and its mouse ortholog with a separation of the two by a slash (human/mouse). IE, immediate-early; LR, late response; Tra, transient upregulation; Sus, sustained upregulation; Amp, amplified upregulation; NA, not applicable; *Hs*, upregulated hiPSCd neuron-specifically; com, upregulated in hiPSCd neurons and in mouse neurons. Each genes' status in regard to neuron-enriched open chromatin-associated promoter mark (Neuron enr.) and human-specific promoter or enhancer epigenetic regulatory gain (*Hs*-sp. gain) in the human brain *in vivo* (see main text for details) is indicated. (P) specifies promoter gain. The asterisk indicates that there is no ortholog in rodents. Mean gene expression level changes (log_2 fold change, log_2FC, determined with RNA-Seq; n = 4 or n = 3, for one hour or four hours of Bic/4AP-treatment, respectively) were used to generate the heat map together with Euclidean distance Ward clustering.

Table S1 (Excel worksheet). Related to Experimental Procedures
(Table S1A) Results of the ToppGene Suite analysis of GO category over-representation among genes more than 8-fold upregulated after generation of NPCs from iPSCs and 7 weeks of neuronal differentiation of NPCs (2106 genes).
(Table S1B) Results of the ToppGene Suite analysis of GO category over-representation among genes more than 8-fold downregulated after generation of NPCs from iPSCs and 7 weeks of neuronal differentiation of NPCs (2105 genes).

Table S2 (Excel worksheet). Related to Figure 4
(Table S2A) DESeq2 results showing human genes with significantly ($p_{adj} < 0.1$) changed RNA expression levels in response to one hour of Bic/4AP-treatment of 7 weeks differentiated hiPSCd neurons in co-culture with mouse primary hippocampal neurons.
(Table S2B) DESeq2 results showing human genes with significantly ($p_{adj} < 0.1$) changed RNA expression levels in response to one hour of Bic/4AP-treatment of 10 weeks differentiated hiPSCd neurons.

Table S3 (Excel worksheet). **Human synaptic activity-regulated immediate early genes.** Related to Figure 4
Shown are DESeq2 results for human IE genes in response to one hour of Bic/4AP-treatment of 7 weeks differentiated hiPSCd neurons in co-culture with mouse primary hippocampal neurons.

Table S4 (Excel worksheet). Results of the ToppGene Suite analysis of GO category and transcription factor binding site over-representation among human synaptic activity-regulated IE genes. Related to Figure 4

Table S5 (Excel worksheet). Related to Figure 6
(Table S5A) DESeq2 results showing human genes with significantly ($p_{adj} < 0.1$) changed RNA expression levels in response to four hours of Bic/4AP-treatment of 7 weeks differentiated hiPSCd neurons in co-culture with mouse primary hippocampal neurons.
(Table S5B) DESeq2 results showing human genes with significantly ($p_{adj} < 0.1$) changed RNA expression levels in response to four hours of Bic/4AP-treatment of 10 weeks differentiated hiPSCd neurons.

Table S6 (Excel worksheet). **Human synaptic activity-regulated late response genes.** Related to Figure 6
Shown are DESeq2 results for human late response genes in response to one hour of Bic/4AP-treatment of 7 weeks differentiated hiPSCd neurons in co-culture with mouse primary hippocampal neurons.

Table S7

hiPSCd n.-specific LR genes	FC *Hs* (+*Mm*)	FC *Hs* (-*Mm*)	neuron-enriched	*Hs* -specific gain
RTL1	4.36	2.26	no	no
RASGRP3	3.79	2.14	no	yes(promoter)
AGPAT9 (*GPAT3*)	3.07	2.11	yes	no
DIO3	2.92	2.56	no	yes(promoter)
TNFRSF9	2.64	4.08	no	no
NAB2	2.36	1.55	yes	no
ADRA1B	2.35	2.11	yes	yes
NKD2	1.86	1.52	yes	yes
F2RL1	1.77	1.43	no	no
CALCB	1.67	2.65	no	yes(promoter)
NPHP4	1.67	1.41	yes	yes
CEMIP	1.65	3.05	yes	no
DNMBP	1.60	1.24	yes	no
TUNAR	1.59	1.59	yes	no
PRPF4	1.47	1.27	no	no
CAMTA1	1.47	1.34	yes	yes
MAK16	1.39	1.32	no	no
ZNF330	1.36	1.26	no	no
ATG16L1	1.36	1.31	yes	no
POLD3	1.35	1.35	no	yes
GORASP1	1.31	1.22	yes	no
CPOX	1.29	1.41	yes	no
FAM134C	0.79	0.81	yes	yes
SORBS2	0.77	0.78	yes	yes
PLCH1	0.73	0.73	no	no
JMY	0.72	0.74	yes	yes
ARID5B	0.70	0.69	no	no
CNTN3	0.69	0.71	no	no
DNAJC27-AS1[a]	0.64	0.59	no	no
RTP1	0.61	0.46	no	no
TMEM187[a]	0.57	0.70	yes	yes

[a]no ortholog in rodents

Table S7. hiPSCd neuron-specifically synaptic activity-regulated late response genes. Related to Figure 6
31 human late response (LR) genes detected here to be significantly regulated by synaptic activity only in hiPSCd neurons (hiPSCd n.) without published evidence for neuronal activity-dependent regulation of the mouse ortholog. Mean expression level changes (fold change, FC, determined with RNA-Seq) in response to four hours of Bic/4AP-treatment of the hiPSCd neuron/mouse primary neuron co-culture [*Hs*(+*Mm*)] and the hiPSCd neuron-only culture [*Hs*(-*Mm*)] is shown. Each genes' status in regard to neuron-enriched open chromatin-associated promoter mark (neuron-enriched) and human-specific promoter or enhancer epigenetic regulatory gain (*Hs*-specific gain) is indicated, (promoter) indicates promoter gain (see main text for details).

Supplemental Experimental Procedures

Human iPSCs. Both iPSC lines used in this study, hiPS D1 (Horschitz et al., 2015) and iPS 3 (Utikal et al., 2009), have been fully characterized to be pluripotent by standard methods, including teratoma formation assay. In this study, if not indicated otherwise, experiments were performed with hiPS D1-derived neurons.

Generation of NPCs. iPSC colonies, grown on Matrigel (BD Biosciences) in mTesR1 (STEMCELL Technologies), were pretreated with the ROCK inhibitor Y-27632 (10 µM, EMD Millipore) and dissociated with Accutase (eBioscience). 10,000 cells were aggregated to form embryoid bodies (EBs) in V-bottom 96-well plates (Thermo Fisher Scientific) by centrifugation at 400 RCF in mTeSR1 with Y-27632 (30 µM). After 16 h EBs were transferred into neural induction (NI) medium [DMEM:F12, Glutamax (2 mM), N2 (1 %), B27 -vitamin A (4%), β-mercaptoethanol (50 µM) (all Thermo Fisher Scientific), Dorsomorphin (500 nM, Tocris), recombinant mouse Noggin (100 ng/mL, R&D Systems), SB431542 (10 µM, Tocris) and Pen/Strep (Thermo Fisher Scientific, 1:200)] as free floating EBs for two days. Then, the EBs were plated onto Matrigel-coated dishes in NI medium with FGF2 (20 ng/mL, PeproTech). After four days, neural rosettes were microdissected from EBs and replated onto Matrigel in NI medium with FGF2 for another four days. Until this stage the medium was changed every day. Then, cells were treated with Accutase and replated as a monolayer on poly-ornithine (0.1 mg/mL) and laminin (10 µg/mL) coated (PO/Lam, both Sigma Aldrich) dishes in NI medium with FGF2. After two days, or when fully confluent, cells were Accutase-treated and split 1:3 onto PO/Lam dishes in NPC medium [DMEM:F12, Glutamax (2 mM), N2 (1 %), B27 -vitamin A (2 %), β-mercaptoethanol (50 µM), Pen/Strep (1:200), EGF (10 ng/mL) (all Thermo Fisher Scientific) and FGF2 (10 ng/mL, PeproTech)]. These cells were termed passage 1 (P1) NPCs. NPCs were maintained on PO/Lam dishes in NPC medium, split 1:3 or 1:4 with Accutase when confluent and used for neuronal differentiation at passage 4 to 10. NPCs can be frozen in NPC medium without Pen/Strep in the presence of 10 % DMSO.

Neuronal differentiation. When plating cells to differentiate, CHIR99021 (2.5 µM, Cellagen Technology) was added to the NPC medium without EGF and FGF2 to increase viability of cells. Cells were maintained in this medium for 7 days with full medium change every other day. Then, cells were treated with Accutase and replated 75,000 cells/cm^2 on PO/Lam dishes or coverslips in neuronal differentiation (ND) medium [Neurobasal (Thermo Fisher Scientific), Glutamax (1 mM), B27 -vitamin A (2 %), ascorbic acid (200 µM, Sigma Aldrich), Pen/Strep (1:200) and BDNF (10 ng/mL, PeproTech)] and allowed to differentiate for up to 9 more weeks with full medium changes three times per week. NPCs differentiated for 7 days can be frozen in NPC medium without EGF, FGF2 and Pen/Strep in the presence of 10 % DMSO, re-thawed and plated into ND medium to differentiate.

hiPSCd neuron/mouse primary hippocampal neuron co-culture. All medium was changed at mouse cell day *in vitro* (DIV) 1, 3, 6 and half of the medium was changed at DIV 8.

Lentivirus production. 60 % confluent HEK293FT (Invitrogen) cells on a 15 cm cell culture dish in high glucose DMEM (Thermo Fisher Scientific), supplemented with 10 % heat-inactivated fetal bovine serum (Thermo Fisher Scientific), non-essential amino acids (Thermo Fisher Scientific, 1:100) and sodium pyruvate (Thermo Fisher Scientific, 1:100), were transfected with plasmids pLP1 (11 µg), pLP2 (5.75 µg), pVSVG (6.5 µg) and pRRL (17.75 µg) (Follenzi et al., 2000) containing either EGFP or mCherry under the control of the human *SYN1* promoter using Lipofectamine 2000 (Thermo Fisher Scientific) according to the manufacturer's instructions. DNA (µg):Lipofectamine 2000 (µl) ratio of 1:2.5 in a total of 625 µl DMEM was used for preparing the transfection solution. Medium was changed 16 h after transfection. Then, the medium was collected twice after 24 h and 48 h. After centrifugation (4 °C, 2500 × g, 10 min) the collected medium was filtered (0.45 µm pore, PVDF, Millex-HV, Merck Millipore), purified (Speedy Lentivirus Purification, abm) and concentrated (Amicon-Ultra 100K column, Merck Millipore), all according to the manufacturer's recommendations, respectively. Viral particles in PBS were aliquoted and frozen in a cell freezing container for storage at -80 °C.

NPC infection. 75 % confluent NPCs (P2 to P4) were infected overnight with the addition of a 1:500 dilution of concentrated lentivirus into NPC medium. Infected NPCs were used for neuronal differentiation after no more than two passages.

Immunocytochemistry. Cells grown on glass coverslips for the time indicated were fixed with 4 % PFA/4 % sucrose in PBS, treated with 50 mM NH_4Cl in PBS, permeabilized with 0.25 % – 0.5 % Triton X-100 in PBS (or with 0.1 % saponin in PBS if anti-VGLUT2 was used, then all subsequent solutions contained 0.1 % saponin), blocked with ICC

blocking buffer (2 % BSA in PBST) and incubated with the following primary antibodies diluted in ICC blocking buffer: goat anti-BRN2 (C-20) (Santa Cruz Biotechnology, sc-6029, 1:50), mouse anti-COUP-TFI [H8132] (Abcam, ab41858 1:200), goat anti-DCX (C18) (Santa Cruz Biotechnology, sc-8066, 1:100), rabbit anti-FOXP2 (Abcam, ab16046, 1:400), rabbit anti-GABA (Sigma-Aldrich, A2052, 1:2000), rabbit anti-JUNB (C37F9) (Cell Signaling Technology, #3753, 1:200), mouse anti-MAP2 (Millipore, MAB3418, 1:500), mouse anti-NES (10C2) (Millipore, MAB5326, 1:400), goat anti-OCT4 (N-19) (Santa Cruz Biotechnology, sc-8628, 1:100), rabbit anti-PAX6 (Covance, PRB-278P, 1:200), mouse anti-TUBB3 (Covance, MMS-435P, 1:500) and rabbit anti-VGLUT2 (Synaptic Systems, 135 402, 1:500). Dylight488- or Dylight594-conjugated anti-IgG secondary antibodies, all produced in donkey by Dianova (anti-goat, 705-515-003; anti-mouse, 715-485-150; or anti-rabbit 711-585-152) were diluted in ICC blocking buffer 1:1000. Coverslips were mounted using Mowiol 4-88 (Merck Millipore) with Hoechst 33258 (Serva). Images were obtained with DM IRB/E inverted microscope (Leica) with a 40× objective, or with TCS SP2 confocal laser-scanning microscope (Leica) equipped with DM IRE2 inverted microscope (Leica) with a 100× objective (JUNB immunostainings).

RNA isolation, cDNA synthesis, RT-PCR and RT-qPCR. At the time of differentiation indicated and/or after the treatment specified, total RNA was purified from cultured cells (3.5 cm dish) with RNeasy Mini (hiPSCd neuron/mouse primary neuron co-cultures) or Micro (hiPSCd neuron-only cultures) Kit (Qiagen) along with on-column RNase-Free DNase (Qiagen) digestion of DNA according to manufacturer's instructions. cDNA was produced with SuperScript III Reverse Transcriptase (Thermo Fisher Scientific) using 100 - 1000 ng of total RNA. Semiquantitative RT-PCR was performed with NEB Taq DNA Polymerase (New England Biolabs). RT-qPCR analysis was performed in triplicates with Power SYBR Green Master Mix (Thermo Fisher Scientific) and 7300 Real-Time PCR System (Applied Biosystems). *TBP* and *GAPDH* or *Gapdh* were used for expression normalization in hiPSCd neuron differentiation and synaptic activity-regulated transcription experiments, respectively. All primers used here are listed in a table available at the end of the Supplemental Experimental Procedures.

Western blotting. Cells grown on 3.5 cm dishes for the time indicated were washed once with ice-cold PBS, collected and pelleted in PBS at 4 °C and lysed on ice in RIPA buffer (50 mM Tris pH 8, 150 mM NaCl, 1 % Triton X-100, 0.5 % Na-deoxycholate and 0.1 % SDS, supplemented with 1 mM PMSF and 1× Roche complete EDTA-free protein inhibitor cocktail) for 30 min. After centrifugation with a table-top centrifuge at 4 °C with 13,000 rpm for 10 min, the supernatant was collected on ice. 50 µg of protein/sample was separated in 10 % SDS-PAGE and transferred to nitrocellulose blotting membrane (GE Healthcare). Membranes were blocked in blocking buffer (5 % skim milk in PBST). The primary antibodies used and their dilutions in blocking buffer applied were: mouse anti-ACTB (Santa Cruz Biotechnology, sc-47778, 1:2000), mouse anti-COUP-TFI [H8132] (Abcam, ab41858 1:800), mouse anti-DLG3 (N19-2) (antibodies-online, ABIN1304941, 1:2000), mouse anti-MAP2 (Millipore, MAB3418, 1:2000), mouse anti-NES (10C2) (Millipore, MAB5326, 1:2000), goat anti-SOX2 (Y-17) (Santa Cruz Biotechnology, sc-17320, 1:400), mouse anti-TUBB3 (Covance, MMS-435P, 1:2000) and rabbit anti-VAMP2 (anti-Synaptobrevin 2) (Synaptic Systems, 104202, 1:2000). HRP-conjugated anti-IgG secondary antibodies used, diluted in blocking buffer 1:5000, were from Dianova: donkey anti-goat (705-035-147), goat anti-mouse (115-035-003) or goat anti-rabbit (111-035-144). Chemiluminescence, produced with the ECL Western Blotting Detection system (GE Healthcare), was detected by exposing membranes to High Performance Chemiluminescence film (GE Healthcare).

RNA-Seq. Poly(A)+ RNA was isolated from total RNA with the NEBNext Poly(A) mRNA Magnetic Isolation Module (New England Biolabs). cDNA libraries were prepared with NEBNext Ultra Directional RNA Library Prep Kit for Illumina (New England Biolabs). NEBNext Multiplex Oligos for Illumina (New England Biolabs) were used. All the preparatory work was performed by CellNetworks Deep Sequencing Core Facility in Heidelberg, Germany. The libraries were sequenced in EMBL Genomics Core Facility in Heidelberg, Germany, on HiSeq 2000 or NextSeq 500 (Illumina) to generate 50 bp single-end reads for iPSC and 7 weeks- or 10 weeks-differentiated hiPSCd neuron samples and 50 bp or 75 bp paired-end reads for 7-weeks-differentiated hiPSCd neuron/mouse primary neuron co-culture samples.

Differential gene expression analysis. Before the final read alignment and differential gene expression analysis, in order to discriminate human and mouse reads, the sequencing data from hiPSCd neuron/mouse primary neuron co-culture samples was processed similar to what has been described for tumour xenograft RNA-Seq data analysis (Bradford et al., 2013). Paired-end reads were aligned independently, without pairing, to either the human genome assembly GRCh37/hg19 or to the mouse genome assembly GRCm38/mm10 with Bowtie2 version 2.1.0 (Langmead and Salzberg, 2012). Unaligned read pairs were joined and split again (Blankenberg et al., 2010) to eliminate pairs

with one aligned read. Then, genome-unaligned paired-end reads were aligned to either GRCh37/hg19 or GRCm38/mm10 transcriptomes (UCSC Genes/knownGene), respectively, with Bowtie2 (2.1.0). The reads that were not aligned to the human genome and transcriptome, or not aligned to the mouse genome and transcriptome, were then handled as reads obtained from single-species samples and used as mouse or human RNA-seq data input to TopHat, respectively. Both, processed mixed-species sample reads and human-cells-only sample reads, were aligned to gene model annotations of the human genome assembly GRCh37/hg19 (or, if appropriate, the mouse genome assembly GRCm38/mm10) with TopHat version v2.0.9 (Kim et al., 2013). Mapped reads per gene were counted strand-specifically with HTSeq-count (HTSeq version 0.6.0 or 0.6.1) in the union overlap resolution mode (Anders et al., 2015). All aligning and counting were done via the Galaxy platform (Goecks et al., 2010; http://usegalaxy.org/; http://galaxeast.fr/). Differentially expressed genes were determined with the DESeq2 package version 1.8.1 (Love et al., 2014) in R (3.2.1) environment (http://www.R-project.org/). Cook's distance flagging functionality was disabled. Benjamini-Hochberg adjusted $p < 0.1$ was considered significant for synaptic activity-regulated gene expression analysis.

Spearman correlation between transcriptomes. Analysis was performed using R (3.2.1). Gene expression levels in RNA-seq read counts per million were used to compare datasets. Counts with added pseudocount of 1 were log-transformed. 4497 genes with variable expression levels between samples, defined by standard deviation > 1 within all samples shown in Figure 1K, were used to calculate Spearman correlation coefficients.

Hierarchical clustering. Size factor normalized RNA-Seq counts from not treated and one hour and four hours Bic/4AP-treated samples were scaled per gene in the range of 0 to 1, and used to compute a Euclidean distance matrix. Agglomerative hierarchical clustering was performed using R (3.2.1) with Ward's clustering criterion (method *ward.D2*).

GO term enrichment analyses. Over-represented GO terms within gene lists were acquired with ToppGene (Chen et al., 2009).

Patch clamp recordings. Cells were viewed with differential interference contrast optics and infrared illumination through a 40x objective (LUMPLFL40xW, N.A. 0.8, Olympus) on a wide field upright microscope (BX51WI, Olympus) equipped with a digital camera (sCMOS, Andor, BFi OPTiLAS) connected to a computer monitor through a PC interface using Andor IQ2 software. $EGFP^+$ or $mCherry^+$ cells were identified using appropriate LEDs (CoolLEDs, Andover, UK) and filters (AHF Analysetechnik). Patch electrodes (3-4 MΩ) were made from borosilicate glass (1.5 mm, WPI) and filled with intracellular solution [HEPES pH 7.35 (10 mM), KGluconate (122 mM), KCl (12 mM), NaCl (8 mM), EGTA (5 mM), $CaCl_2$ (0.25 mM), Na_3-GTP (0.5 mM), Mg_2-ATP (4 mM), K2-phosphocreatine (10 mM)]. Extracellular solution was an artificial cerebrospinal fluid, ACSF [NaCl (125 mM), KCl (3.5 mM), $MgCl_2$ (1.3 mM), NaH_2PO_4 (1.2 mM), $CaCl_2$ (2.4 mM), glucose (25 mM), $NaHCO_3$ (26 mM), gassed with 95 % O_2 and 5 % CO_2]. Whole-cell patch clamp recordings were made with a Multiclamp 700A amplifier, digitised through a Digidata 1322A A/D converter and acquired using pClamp 10 software (Molecular Devices). Spontaneous postsynaptic currents were recorded in voltage clamp at a -70 mV holding potential. Stock solutions of Bic (Enzo Life Sciences) were dissolved in DMSO and gabazine-hydrobromide (SR95531, Biotrend), 4AP (Sigma), 2,3-dioxo-6-nitro-1,2,3,4-tetrahydrobenzo[f]quinoxaline-7-sulfonamide disodium salt (NBQX, Biotrend) and TTX (Biotrend) in water. Cell numbers are given in the figures and their legends.

Ca^{2+} imaging. For multi-cellular Ca^{2+} imaging experiments, cells were loaded at 36 °C with membrane permeable Rhod2-AM [1.5 µM (stock dissolved at 1.5 mM in pluronic acid and DMSO)] for 30 min followed by 10 min washout for de-esterification of the dye. Somatic Ca^{2+} levels were quantified as $(F-F_{min})/(F_{max}-F)$ where F represents the average fluorescence intensity, F_{max} represents the maximal F after incubation in 50 µM ionomycin, and F_{min} represents the minimal F after subsequent application of a 1:500 dilution of saturated manganese solution.

Nanostring nCounter analysis (Kulkarni et al., 2011). Custom designed nCounter Elements code set targeting human-specifically 30 human genes and mouse-specifically 17 mouse genes was used. Probe sequences are available upon request. The nSolver Analysis Software (version 2.5) was used to analyse RNA expression data produced by CellNetworks nCounter Core Facility in Heidelberg, Germany. Geometric means were used to perform background subtraction, to compute normalization factors for positive control normalization and perform code set content

normalization. Count ratio (log_2) was used for assessing differential expression between the analysed conditions with one-way ANOVA and Dunnett's multiple comparisons tests.

Luciferase reporter assays. Human *BRE-AS1*, *LINC00473* and *ZNF331* and mouse *Hic1* genomic proximal promoter sequences were PCR-amplified (Phusion High-Fidelity DNA Polymerase, New England Biolabs), cloned into the pGL4.15[luc2P/Hygro] vector (Promega) and verified by sequencing. *pBRE-AS1* was the only cloned promoter not fully verified by sequencing because of sequencing problems. Instead, it was confirmed to be correct by control cuts with several restriction enzyme combinations. The primers used for amplification of genomic DNA are listed in a table available at the end of the Supplemental Experimental Procedures. pGL4.29[luc2P/CRE/Hygro] (Promega), containing four CRE *cis*-elements and a minimal promoter (4×CRE-pmin), and pGL4.15[luc2P/Hygro]/p*BDNF* IV, containing the human *BDNF* promoter IV (Pruunsild et al., 2011), or pGL4.15[luc2P/Hygro] (Promega) without promoter (pCNTR), were used as positive or negative controls, respectively, for synaptic activity-induced transcriptional activity. pGL4.83[hRlucP/Puro] plasmid containing the human *EF1α* promoter in front of Renilla luciferase (Rluc) (Sepp et al., 2012) was used for normalization. At DIV 8 mouse (P0) primary hippocampal or cortical neurons in 48-well plates, maintained thus far in Neurobasal-A supplemented with rat serum (1 %), B27 (2 %), L-glutamine (0.5 mM) and Pen/Strep (1:200) (all Thermo Fisher Scientific), were changed to transfection medium (TM) consisting of salt-glucose-glycine solution [HEPES pH 7.4 (10 mM), NaCl (114 mM), $NaHCO_3$ (26.1 mM), KCl (5.3 mM), $MgCl_2$ (1 mM), $CaCl_2$ (2 mM), glycine (1 mM), glucose (30 mM), sodium pyruvate (0.5 mM) and phenol red (0.001 %)] and minimum Eagle's medium (with Earle's salt and without L-glutamine, Thermo Fischer Scientific), 9:1; supplemented with insulin (6.3 µg/mL), transferrin (5.7 µg/mL) and sodium selenite (7.5 ng/mL) (ITS, Sigma Aldrich). Lipofectamine 2000 (Thermo Fisher Scientific) was used for transfection at DIV 8 according to the manufacturer's instructions. Cells were transfected with a pGL4.15[luc2P/Hygro] plasmid (Promega) containing the indicated cloned promoter in front of FFluc, or with the pGL4.29[luc2P/CRE/Hygro] plasmid, or the pGL4.15[luc2P/Hygro] plasmid (both Promega) (all 0.5 µg/well), together with the pGL4.83[hRlucP/Puro] plasmid containing the human *EF1α* promoter in front of Renilla luciferase (Rluc) (5 ng/well) for normalization. If mCherry, CaMBP4, ICER or delTAD-NPAS4 was co-expressed, 0.25 µg/well of either pmCherry-N1 (Clontech), rAAV/CaMBP4-mCherry (Lau and Bading, 2009), pcDNA3.1/ICER (Pruunsild and Timmusk, 2012) or pcDNA3.1/delTAD-NPAS4 (Pruunsild et al., 2011), respectively, along with 0.25 µg/well of FFluc construct and 5 ng/well of Rluc construct were co-transfected. DNA (µg):Lipofectamine 2000 (µl) ratio of 1:2 in total of 25 µl/well TM was used for preparing the transfection solution. At DIV 10, Dual-Glo Luciferase Assay System (Promega) was used to measure FFluc and Rluc levels. Background measured from non-transfected cells was subtracted and FFluc levels were normalized to Rluc levels. Data presented in Figure 5B were autoscaled using the data obtained with the pGL4.29[luc2P/CRE/Hygro] construct. All data presented as fold change after Bic/4AP-treatment was log-transformed for statistical analyses.

Gene classification based on promoter/enhancer histone modifications. Data for neuron-enriched H3K4me3 promoter marks in the human prefrontal cortex *in vivo* is from Cheung et al. (Cheung et al., 2010) and for human-specific promoter or enhancer H3K27ac and/or H3K4me2 gains during brain cortex development *in vivo* is from Reilly et al. (2015). UMMS Brain Hist Track and 8 custom tracks with peaks for human-specifically increased H3K27ac or H3K4me2 marks in the human cortex at postconception week (pcw) 7 or 8.5, and in the frontal or occipital cortex at pcw 12 (Reilly et al., 2015) were used to display data in the UCSC Genome Browser. We assigned a gene to have a neuron-enriched H3K4me3 promoter mark if according to the data by Cheung *et al*. the mark was enriched in all neuronal samples compared with lymphocyte samples and overlapped a TSS. We categorized a gene to have a human-specific epigenetic promoter gain if in at least two of the total of 8 ChIP-Seq tracks with peaks for human-specifically increased H3K27ac or H3K4me2 marks (Reilly et al., 2015), the peaks were coinciding and overlapped a TSS. A gene was considered to have a human-specific epigenetic enhancer gain if it was located in a gain-enriched genomic hotspot (Reilly et al., 2015), and/or in at least two of the 8 tracks with human-specifically increased H3K27ac or H3K4me2 ChIP-Seq peaks, the peaks were coinciding and not overlapping a TSS, but were within 30,000 bps up- to 15,000 bps downstream of any of the TSSs of the gene, and were not in an adjacent gene. Exceptionally, the gain mark inside an adjacent gene was counted if the gene of interest and the adjacent gene had a bidirectional, "head-to-head" promoter. RefSeq genes (as in Cheung et al., 2010) and Genecode version 10 genes (as in Reilly et al., 2015) were used to estimate chance levels of the respective promoter marks. A set of 85 random genes were included in the comparison of proportions of genes with human-specific epigenetic enhancer gains between different gene sets.

Statistical analyses. t-tests and ANOVA were performed using GraphPad Prism or Origin. For statistical analysis qPCR, nCounter and luciferase assay data were log-transformed and cell proportions obtained with immunocytochemistry were arcsine-transformed. Exact binomial tests and Fisher's pairwise comparisons of proportions with Holm's p adjustment were performed using R (3.2.1).

Primers used in this study

Target	Sense	Antisense	Amplicon (bps)
		Expression	
OCT4	GGGAAGGTATTCAGCCAAAC	CTTTCTCTTTCGGGCCTGCAC	174
PAX6	GCACCAGTGTCTACCAACCAA	CCCAACATGGAGCCAGATGTGAA	73
BRN1	TTGGCGCTGGGCACACTCTA	CCTTGACGCTCACCTCGATAG	223
RTN1	ACGGGCATCGTGTTTGGGAGT	TGCCTCTTAGCGCCTGGGATT	521
STMN2	GCTCTTGCTTTTACCCGGAAC	ATTGTTTCAGCACCTGGGCCT	219
TBP	GCCTTGTGCTCACCCACCAACAATTT	GGTACATGAGAGCCATTACGTC	221
CUX1	CAAAGGCCAGGCTGACTATGA	TCTCCAGCAACAGCACCTCCA	128
LIN28A	GAGGCGGCCAAAAGGAAAGAG	ATTCCTTGGCATGATGATCTAGACCT	92
SOX1	CGCTGACACCAGACTTGGGTT	ACAAAAGTGGGCTTCGCCTCT	154
SYN1	GGAGAAATTGACATTAAAGTAGAACAG	CTTCTGTCCCCAGTTTCTTATGC	319
NPAS4 (*Hs*)	GTGAGGCTACAGGCCAAGAC	AGGGCAGCATGGTCGGAGTG	190
Npas4 (*Mm*)	CAGGGCGACAGTATCTACGAT	CAACGGAAAAGGCGATCAGCA	104
FOS (*Hs*)	TGCAGCCAAATGCCGCAAC	TCGGTGAGCTGCCAGGATG	154
Fos (*Mm*)	GGCAGAAGGGGCAAAGTAGAG	TGTCAGCTCCCTCCTCCGATTC	117
ARC (*Hs*)	AAGTCGCACACGCAGCAGAGCA	AGGCGGGCGTGAATCACTGGA	77
Arc (*Mm*)	AGACCTGACATCCTGGCACC	GCTCTGCTCTTCTTCACTGGTA	65
GAPDH (*Hs*)	CAAAATCAAGTGGGGCGATGCT	TTGGCTCCCCCCTGCAAATGA	102
Gapdh (*Mm*)	CACTCTTCCACCTTCGATGCC	GGGTGGGTGGTCCAGGGTT	159
HIC1 (*Hs*)	ATGCGGTTCACGCGCCAGTAC	CTGATGAGGTTGCGTTGCTGT	116
Hic1 (*Mm*)	ATGCGCTTCACCCGCCAGTAT	CTGATGAGGTTGCGCTGTTGA	116
		Promoter	
p*BRE-AS1* (BglII)	ACGTACAGATCTGATGACACCTGAGGGAATGAA	ACGTACAGATCTAAGTTCCAGGTACCTGGACTG	1024
p*LINC00473* (BglII)	ACGTACAGATCTTGGCCTCTTAAGGGTCTTTTG	ACGTACAGATCTGGCGAGTGTGTGGGGTTCCTC	974
p*ZNF331 I* (BglII)	ACGTACAGATCTTGAACCACTTTTCCCAGGAAT	ACGTACAGATCTGCGTAGAGCCTCTCACGTCAC	1524
p*ZNF331 II* (BglII)	ACGTACAGATCTGGACTACCGGGTGCGTCTGCG	ACGTACAGATCTTCGGGGATGCTTTTTCTGAAG	1524
p*ZNF331 III* (BglII)	ACGTACAGATCTGCGTGTCAGGATCTGTGTGCA	ACGTACAGATCTTTTAACGATTCGTCTTCCTCC	1448
p*Hic1* (*Mm*, HindIII)	ACGTACAAGCTTTCTCCTGCCAAAGAAACGCAGC	ACGTACAAGCTTTGCCGGCGGATCCAGGGGGGGA	1677
		Mutagenesis	
p*Hic1* (*Mm*, +EGR1 site)	GTCAGGAGGTGCGGGGCGGAGGCGGAGCGTGGGC	GCCCACGCTCCGCCTCCGCCCCGCACCTCCTGAC	

Supplemental References

Anders, S., Pyl, P.T., and Huber, W. (2015). HTSeq--a Python framework to work with high-throughput sequencing data. Bioinformatics *31*, 166-169.

Blankenberg, D., Gordon, A., Von Kuster, G., Coraor, N., Taylor, J., Nekrutenko, A., and Galaxy, T. (2010). Manipulation of FASTQ data with Galaxy. Bioinformatics *26*, 1783-1785.

Bradford, J.R., Farren, M., Powell, S.J., Runswick, S., Weston, S.L., Brown, H., Delpuech, O., Wappett, M., Smith, N.R., Carr, T.H.*, et al.* (2013). RNA-Seq Differentiates Tumour and Host mRNA Expression Changes Induced by Treatment of Human Tumour Xenografts with the VEGFR Tyrosine Kinase Inhibitor Cediranib. PLoS One *8*, e66003.

Camp, J.G., Badsha, F., Florio, M., Kanton, S., Gerber, T., Wilsch-Brauninger, M., Lewitus, E., Sykes, A., Hevers, W., Lancaster, M.*, et al.* (2015). Human cerebral organoids recapitulate gene expression programs of fetal neocortex development. Proceedings of the National Academy of Sciences of the United States of America *112*, 15672-15677.

Chambers, S.M., Fasano, C.A., Papapetrou, E.P., Tomishima, M., Sadelain, M., and Studer, L. (2009). Highly efficient neural conversion of human ES and iPS cells by dual inhibition of SMAD signaling. Nature biotechnology *27*, 275-280.

Chen, J., Bardes, E.E., Aronow, B.J., and Jegga, A.G. (2009). ToppGene Suite for gene list enrichment analysis and candidate gene prioritization. Nucleic Acids Res *37*, W305-311.

Cheung, I., Shulha, H.P., Jiang, Y., Matevossian, A., Wang, J., Weng, Z., and Akbarian, S. (2010). Developmental regulation and individual differences of neuronal H3K4me3 epigenomes in the prefrontal cortex. Proceedings of the National Academy of Sciences of the United States of America *107*, 8824-8829.

Fietz, S.A., Lachmann, R., Brandl, H., Kircher, M., Samusik, N., Schroder, R., Lakshmanaperumal, N., Henry, I., Vogt, J., Riehn, A.*, et al.* (2012). Transcriptomes of germinal zones of human and mouse fetal neocortex suggest a role of extracellular matrix in progenitor self-renewal. Proceedings of the National Academy of Sciences of the United States of America *109*, 11836-11841.

Follenzi, A., Ailles, L.E., Bakovic, S., Geuna, M., and Naldini, L. (2000). Gene transfer by lentiviral vectors is limited by nuclear translocation and rescued by HIV-1 pol sequences. Nat Genet *25*, 217-222.

Goecks, J., Nekrutenko, A., Taylor, J., and Galaxy, T. (2010). Galaxy: a comprehensive approach for supporting accessible, reproducible, and transparent computational research in the life sciences. Genome Biol *11*, R86.

Horschitz, S., Matthaus, F., Gross, A., Rosner, J., Galach, M., Greffrath, W., Treede, R.D., Utikal, J., Schloss, P., and Meyer-Lindenberg, A. (2015). Impact of preconditioning with retinoic acid during early development on morphological and functional characteristics of human induced pluripotent stem cell-derived neurons. Stem Cell Res *15*, 30-41.

Imaizumi, K., Sone, T., Ibata, K., Fujimori, K., Yuzaki, M., Akamatsu, W., and Okano, H. (2015). Controlling the Regional Identity of hPSC-Derived Neurons to Uncover Neuronal Subtype Specificity of Neurological Disease Phenotypes. Stem cell reports *5*, 1010-1022.

Kim, D., Pertea, G., Trapnell, C., Pimentel, H., Kelley, R., and Salzberg, S.L. (2013). TopHat2: accurate alignment of transcriptomes in the presence of insertions, deletions and gene fusions. Genome Biol *14*, R36.

Kim, J.E., O'Sullivan, M.L., Sanchez, C.A., Hwang, M., Israel, M.A., Brennand, K., Deerinck, T.J., Goldstein, L.S., Gage, F.H., Ellisman, M.H., and Ghosh, A. (2011). Investigating synapse formation and function using human pluripotent stem cell-derived neurons. Proceedings of the National Academy of Sciences of the United States of America *108*, 3005-3010.

Kulkarni, M.M. (2011). Digital multiplexed gene expression analysis using the NanoString nCounter system. Curr Protoc Mol Biol Chapter *25*, Unit25B 10.

Langmead, B., and Salzberg, S.L. (2012). Fast gapped-read alignment with Bowtie 2. Nat Methods *9*, 357-359.

Lau, D., and Bading, H. (2009). Synaptic activity-mediated suppression of p53 and induction of nuclear calcium-regulated neuroprotective genes promote survival through inhibition of mitochondrial permeability transition. J Neurosci *29*, 4420-4429.

Love, M.I., Huber, W., and Anders, S. (2014). Moderated estimation of fold change and dispersion for RNA-seq data with DESeq2. Genome Biol *15*, 550.

Pruunsild, P., Sepp, M., Orav, E., Koppel, I., and Timmusk, T. (2011). Identification of cis-elements and transcription factors regulating neuronal activity-dependent transcription of human BDNF gene. J Neurosci *31*, 3295-3308.
Pruunsild, P., and Timmusk, T. (2012). Subcellular localization and transcription regulatory potency of KCNIP/Calsenilin/DREAM/KChIP proteins in cultured primary cortical neurons do not provide support for their role in CRE-dependent gene expression. J Neurochem *123*, 29-43.
Reilly, S.K., Yin, J., Ayoub, A.E., Emera, D., Leng, J., Cotney, J., Sarro, R., Rakic, P., and Noonan, J.P. (2015). Evolutionary genomics. Evolutionary changes in promoter and enhancer activity during human corticogenesis. Science *347*, 1155-1159.
Sepp, M., Pruunsild, P., and Timmusk, T. (2012). Pitt-Hopkins syndrome-associated mutations in TCF4 lead to variable impairment of the transcription factor function ranging from hypomorphic to dominant-negative effects. Hum Mol Genet *21*, 2873-2888.
Utikal, J., Maherali, N., Kulalert, W., and Hochedlinger, K. (2009). Sox2 is dispensable for the reprogramming of melanocytes and melanoma cells into induced pluripotent stem cells. Journal of cell science *122*, 3502-3510.
Wen, Z., Nguyen, H.N., Guo, Z., Lalli, M.A., Wang, X., Su, Y., Kim, N.S., Yoon, K.J., Shin, J., Zhang, C*., et al.* (2014). Synaptic dysregulation in a human iPS cell model of mental disorders. Nature *515*, 414-418.